The 2010 stock assessment of paua (*Haliotis iris*) for Chalky and South Coast in PAU 5A

D. Fu
A. McKenzie

NIWA
Private Bag 14901
Wellington 6241

New Zealand Fisheries Assessment Report 2010/36
October 2010

Published by Ministry of Fisheries
Wellington
2010

ISSN 1175-1584 (print)
ISSN 1179-5352 (online)

Fu, D.; McKenzie, A.; (2010).
The 2010 stock assessment of paua (*Haliotis iris*) for Chalky and South Coast in PAU 5A.
New Zealand Fisheries Assessment Report 2010/36.

This series continues the informal
New Zealand Fisheries Assessment Research Document series
which ceased at the end of 1999.

EXECUTIVE SUMMARY

Fu, D.; McKenzie, A. (2010). The 2010 stock assessment of paua (*Haliotis iris*) for Chalky and South Coast in PAU 5A.

***New Zealand Fisheries Assessment Report 2010/36*.**

The stock assessments for PAU 5A have previously been carried out at the QMA level. In 2010 the Shellfish Working Group decided to conduct the stock assessment for the two subareas of PAU 5A separately: a southern area including Chalky and South Coast, and a northern area including Milford, George, Central, and Dusky. The decision was made in order to address the differences in exploitation histories between subareas within PAU 5A, and to reflect recent changes in management measures of the fishery.

This report summarises the stock assessment for the southern area of PAU 5A with the inclusion of fishery data from Chalky and South Coast up to 2008–09 fishing year. The report describes the model structure and output, including current and projected stock status. The stock assessment is implemented as a length-based Bayesian estimation model, with point estimates of parameters based on the mode of the joint posterior distribution, and uncertainty of model estimates investigated using the marginal posterior distributions generated from Markov chain-Monte Carlo simulation.

The model dynamics used for this assessment are similar to those of the previous assessment, with minor modifications to accommodate the changes in the minimum harvest size. The data fitted in the assessment model were: (1) a standardised CPUE series based on the early CELR data, (2) a standardised CPUE series covering based on recent PCELR data, (3) a standardised research diver survey index (RDSI), (4) a research diver survey proportions-at-lengths series, (5) a commercial catch sampling length frequency series, (6) tag-recapture length increment data, and (7) maturity-at-length data.

The catch history used as the model input included commercial, recreational, customary, and illegal catch. The commercial catch history estimates were made under assumptions concerning the split of the catch between substocks of PAU 5, and between subareas within PAU 5A. The base case model run has assumed 40% of the catch in Statistical Area 030 was taken from PAU 5A between 1985 and 1996. Estimates made under alternative assumptions (a lower bound of 18% and an upper bound of 61%) were used in sensitivity trials.

The maturity and growth data included in the model were based on samples collected throughout PAU 5A, and the abundance and length frequency data were from Chalky and South Coast. The CPUE indices between 1990 and 2001 were based on catch effort data from Statistical Area 030. Only four years of catch sampling length frequencies (2002–2005) were included in base case, as the sampling coverage is low since then and dubious before then. The additional catch sampling data were used in sensitivity trials.

Iterative re-weighting of the datasets produced a base case result in which the standard deviations of the normalised residuals were close to unity for most datasets. The model estimates of the state of the stock in Chalky and South Coast suggest there has been a dramatic reduction of vulnerable abundance as the fishery developed, but the stock shows signs of recovery over the last three years. Current estimates from the base case model run suggested that spawning stock population in 2009 (B_{current}) was about 35% (28–42%) B_0, and recruit-sized stock abundance ($B^r_{current}$) was about 24% (19–29%) of initial state (B^r_0). The model projections, made for three years assuming current catch levels and using recruitments re-sampled from the recent model estimates suggested the stock abundance will continue to increase over the next three years and the projected status of spawning stock biomass in 2012 is projected to be about 39% (30–50%) B_0

The model presented here, whilst fairly representing some of the data, also shows some indications of lack of fit. It is unlikely the estimates of historical stock size are reliable, given assumptions about annual recruitment and the use of the historical catch-effort indices of abundance. The research diver survey indices were fitted poorly, and the inter-annual variability of the indices can not be explained by the model. The model suggested likely conflicts between the CPUE and the catch sampling length frequency (CSLF) when all of the commercial catch length frequency samples were included.

Model fits to abundance indices and estimates of stock status are sensitive to the assumptions made for the commercial catch estimates. With the three alternative catch estimates considered in this assessment, model estimates of $B_{current}$ ranged from 30 to 52% of $B_{0.}$

1. INTRODUCTION

1.1 Overview

PAU 5A was last assessed in 2006 (Breen & Kim 2007) and before that in 2004 (Breen & Kim 2004b). The previous stock assessments for PAU 5A have been conducted assuming a homogeneus area covering the whole PAU 5A.

There have been concerns regarding the applicability of the assessment to the entire QMA, although there was general agreement that biomass decline had occurred in the southern region of the QMA over recent years. Recent studies suggested that trends in the changes of abundance may have varied between subareas within PAU 5A (Cordue 2009). Therefore a model assuming a homogeneus area is unlikely to reflect the different exploitation histories between subareas, or to predict the current status of the stock.

Since 1 October 2006, a voluntary subdivision was agreed which divided PAU 5A into six fishing management zones, based on the research strata, and a proportion of the total annual catch entitlements (ACE) was allocated to each zone. Each of the management zones has a voluntary harvest cap and minimum harvest length in place.

The Shellfish Working Group (SFWG) suggested conducting the 2010 assessment for two subareas of PAU 5A separately: the southern strata including Chalky and South Coast, and the northern strata including Milford, George, Central, and Dusky. The choice was tentatively based on availability of data, differences in exploitation history, and management initiatives.

This report summarises the stock assessment for the southern strata of PAU 5A (Chalky and South Coast) with the inclusion of fishery data up to the 2008–09 fishing year. The stock assessment is made with the length-based Bayesian estimation model first used in 1999 for PAU 5B (Breen et al. 2000a) and revised for subsequent assessments in PAU 5B (Breen et al. 2000b) and PAU 7 (Andrew et al. 2000, Breen & Kim 2003, 2005, McKenzie & Smith 2009) with revisions made for PAU 4 (Breen & Kim 2004a) and PAU 5A (Breen & Kim 2004b) in 2004 mostly discarded. The model was published by Breen et al. (2003).

The seven sets of data fitted in the assessment model were: (1) a standardised CPUE series covering 1990–2001 based on CELR data (CPUE), (2) a standardised CPUE series covering 2002–2009 based on PCELR data (PCPUE), (3) a standardised research diver survey index (RDSI), (4) a research diver survey proportions-at-lengths series (RDLF), (5) A commercial catch sampling length frequency series (CSLF), (6) tag-recapture length increment data, and (7) maturity-at-length data. Catch history was an input to the model, encompassing commercial, recreational, customary, and illegal catch. Another document describes the datasets that are used in the stock assessment and the updates that were made for the previous assessment (Fu et al. 2010).

The assessment was made in several steps. First, the model was fitted to the data with arbitrary weights on the various data sets. The weights were then iteratively adjusted to produce balanced residuals among the datasets where the standardised deviation of the normalised residuals was close to one for each dataset. The fit obtained is the mode of the joint posterior distribution of parameters (MPD). Next, from the resulting fit, Markov chain-Monte Carlo (MCMC) simulations were made to obtain a large set of samples from the joint posterior distribution. From this set of samples, forward projections were made with a set of agreed indicators obtained. Sensitivity trials were explored by comparing MPD fits made with alternative catch history estimates and inclusion of additional CSLF data.

This document describes the model, assumptions made in fitting, the fit of the model to the data, projection results, and sensitivity trials. This report fulfils Objective 1 “To update the stock assessment

for PAU 5A, including estimates of abundance from the fisheries independent dive surveys from Objective 1, in February/March 2010" of Project PAU2007/03.

1.2 Description of the fishery

PAU 5A includes the coastal areas and islands of Fiordland (Figure 1), from Waiau River (west of Riverton) to Awarua Point (north of Big Bay), The TACC for PAU 5A has remained at the initial level of 145 t since the 1995–96 fishing year t. Landings have been close to the TACC since 1998–99 (Ministry of fisheries 2009).

Since 1 October 2006, a voluntary catch reduction of 30% has been in place. The harvest caps are designed to reduce effort in the southern three zones (Dusky, Chalky, and South Coast) and to reduce the catch in these areas by 50%. This effectively reduces the allowable catch from 148 983 to 104 290 kg. Initially the shelving was for 3 years, but at the 2009 PauaMac5 AGM it was agreed to roll this over for another 2 years, reviewable annually.

The paua fishery was summarised by Schiel (1992), and in numerous previous assessment documents (e.g., Schiel 1989, McShane et al. 1994, 1996, Breen et al. 2000a, 2000b, 2001, Breen & Kim 2003, 2004a, 2004b, 2007), and more recently by Fu (unpublished). A further summary is not presented here.

2. MODEL

This section gives an overview of the model used for stock assessment of Chalky and South Coast in 2010; for full details see Breen et al. (2003). The model was developed for use in PAU 5B in 1999 and has been revised each year for subsequent assessments, in many cases echoing changes made to the rock lobster assessment model (Breen et al. 2002, Kim et al. 2004), which is a similar but more complex length-based Bayesian model. Only minor changes were made to the last revision which was the 2008 assessment model of PAU 7 (McKenzie & Smith 2009).

2.1 Changes to the 2008 assessment model of PAU 7

Only one minor change was made, allowing the selectivity to be shifted by 5 mm, echoing a voluntary increase of minimum harvest size change in Chalky and South Coast from October, 2007:

$$V_k^{t,s} = \frac{1}{1+19^{-\left((l_k - D_{50} - E_t)/D_{95-50}\right)}}$$

where $E_t = 0$ for $t < 2007$ or $E_t = 5$ for $t \geq 2007$

Another model change was explored: imposing a penalty function to encourage the average of recruitment deviation to be close to 1. This has only been used to investigate the profile likelihood for one of the sensitivity trials (see later), and was not included for any of the MPD fits.

2.2 Model description

The model partitioned paua stock into a single sex population, with length classes from 70 mm to 170 mm, in groups of 2 mm (i.e., from 70 to under 72 mm, 72 mm to under 74 mm, etc.). The largest length bin is well above the maximum size observed. The stock was assumed to reside in a single,

homogeneous area. The partition accounted for numbers of paua by length class within an annual cycle, where movement between length classes was determined by the growth parameters. Paua entered the partition following recruitment and were removed by natural mortality and fishing mortality.

The model annual cycle was based on the fishing year. Note that model references to "year" within this paper refer to the fishing year, and are labelled as the most recent calendar year, i.e., the fishing year 1998–99 is referred to as "1999" throughout. References to calendar years are denoted specifically.

The models were run for the years 1965–2009. Catches were available for 1974–2009, and were assumed to increase linearly between 1965 and 1973 from 0 to the 1974 catch level. Catches included commercial, recreational, customary, and illegal catch, and all catches occurred at the same time step.

Recruitment was assumed to take place at the beginning of the annual cycle, and length at recruitment was defined by a uniform distribution with a range between 70 and 80 mm. Recruitment deviation were assumed known and equal to 1 for the years up to 1985 — 10 years before the first available length data were available (loosely based on the approximate time taken for recruited paua to appear at the right hand end of the length distribution). The stock-recruitment relationship is unknown for paua, but is likely to be weak or equivocal (Shepherd et al. 2001). A relationship may exist on small scales, but not be apparent when large-scale data are modelled (Breen et al. 2003). No explicit stock-recruitment relationship was modelled in this assessment.

Maturity does not feature in the population partition. The model estimated proportions mature with the inclusion of length-at-maturity data. Growth and natural mortalities were also estimated within the model.

The models used two selectivities: the commercial fishing selectivity and research diver survey selectivity — both assumed to follow a logistic curve (see later). The survey selectivity remained constant, and the commercial fishing selectivity was shifted by 5 cm for 2007–12 (assuming changes in definition of minimum harvest size extend to the projection period).

The model is implemented in AD Model Builder™ (Otter Research Ltd., http://otter-rsch.com/admodel.htm) version 9.0.65, compiled with the MinGW 3.45 compiler.

2.2.1 Estimated parameters

Parameters estimated by the model are as follows. The parameter vector is referred to collectively as θ.

$\ln(R0)$	natural logarithm of base recruitment
M	instantaneous rate of natural mortality
g_α	expected annual growth increment at length α
g_β	expected annual growth increment at length β
ϕ	c.v. of the expected growth increment
q^I	scalar between recruited biomass and CPUE
X	coefficient of proportionality between q^I and q^{I2}, the scalar for PCPUE
q^J	scalar between numbers and the RDSI
L_{50}	length at which maturity is 50%
L_{95-50}	interval between L_{50} and L_{95}

T_{50}	length at which research diver selectivity is 50%
T_{95-50}	distance between T_{50} and T_{95}
D_{50}	length at which commercial diver selectivity is 50%
D_{95-50}	distance between D_{50} and D_{95}
$\tilde{\sigma}$	common component of error
h	shape of CPUE *vs.* biomass relation
ε	vector of annual recruitment deviations, estimated from 1977 to 2004

2.2.2 Constants

l_k	length of a paua at the midpoint of the k^{th} length class (l_k for class 1 is 71 mm, for class 2 is 73 mm and so on)
σ_{MIN}	minimum standard deviation of the expected growth increment (assumed to be 1 mm)
σ_{obs}	standard deviation of the observation error around the growth increment (assumed to be 0.25 mm)
MLS_t	minimum legal size in year t (assumed to be 125 mm for all years)
$P_{k,t}$	a switch based whether abalone in the k^{th} length class in year t are above the minimum legal size (MLS) ($P_{k,t} = 1$) or below ($P_{k,t} = 0$)
a, b	constants for the length-weight relation, taken from Schiel & Breen (1991) (2.592E-08 and 3.322 respectively, giving weight in kg)
w_k	the weight of an abalone at length l_k
ϖ^I	relative weight assigned to the CPUE dataset. This and the following relative weights were varied between runs to find a basecase with balanced residuals
ϖ^{I2}	relative weight assigned to the PCPUE dataset.
ϖ^J	relative weight assigned to the RDSI dataset
ϖ^r	relative weight assigned to RDLF dataset
ϖ^s	relative weight assigned to CSLF dataset
ϖ^{mat}	relative weight assigned to maturity-at-length data
ϖ^{tag}	relative weight assigned to tag-recapture data
κ_t^s	normalised square root of the number measured greater than 113 mm in CSLF records for each year, normalised by the lowest year
κ_t^r	normalised square root of the number measured greater than 89 mm in RDLF records for each year, normalised by the lowest year
$U^{\max}$	exploitation rate above which a limiting function was invoked (0.80 for the base case)
μ_M	mean of the prior distribution for M, based on a literature review by Shepherd & Breen (1992)
σ_M	assumed standard deviation of the prior distribution for M
σ_ε	assumed standard deviation of recruitment deviations in log space (part of the prior for recruitment deviations)

n_ε	number of recruitment deviations
α	length associated with g_α (75 mm)
β	length associated with g_β (120 mm)

2.2.3 Observations

C_t	observed catch in year *t*
I_t	standardised CPUE in year *t*
$I2_t$	standardised PCPUE in year *t*
σ_t^I	standard deviation of the estimate of observed CPUE in year *t*, obtained from the standardisation model
σ_t^{I2}	standard deviation of the estimate of observed PCPUE in year *t*, obtained from the standardisation model
J_t	standardised RDSI in year *t*
σ_t^J	the standard deviation of the estimate of RDSI in year t, obtained from the standardisation model
$p_{k,t}^r$	observed proportion in the k^{th} length class in year *t* in RDLF
$p_{k,t}^s$	observed proportion in the k^{th} length class in year *t* in CSLF
l_j	initial length for the j^{th} tag-recapture record
d_j	observed length increment of the *j*th tag-recapture record
Δt_j	time at liberty for the j^{th} tag-recapture record
p_k^{mat}	observed proportion mature in the k^{th} length class in the maturity dataset

2.2.4 Derived variables

R0	base number of annual recruits
$N_{k,t}$	number of paua in the k^{th} length class at the start of year *t*
$N_{k,t+0.5}$	number of paua in the k^{th} length class in the mid-season of year *t*
$R_{k,t}$	recruits to the model in the k^{th} length class in year *t*
g_k	expected annual growth increment for paua in the k^{th} length class
σ^{g_k}	standard deviation of the expected growth increment for paua in the k^{th} length class, used in calculating $\mathbf{G}$
$\mathbf{G}$	growth transition matrix
B_t	spawning stock biomass at the beginning of year *t*
$B_{t+0.5}$	spawning stock biomass in the mid-season of year *t*
B_0	equilibrium spawning stock biomass assuming no fishing and average recruitment from the period in which recruitment deviations were estimated.
B_{init}	spawning stock biomass at the end of initialisation phase (or B_{1964})
B_t^r	biomass of paua above the MLS at the beginning of year *t*

$B^r_{t+0.5}$	biomass of paua above the MLS in the mid-season of year *t*
B^r_0	equilibrium biomass of paua above the MLS assuming no fishing and average recruitment from the period in which recruitment deviations were estimated
B^r_{init}	biomass of paua above the MLS at the end of initialisation phase (or B^r_{1964})
U_t	exploitation rate in year *t*
A_t	the complement of exploitation rate
$SF_{k,t}$	finite rate of survival from fishing for paua in the *k*th length class in year *t*
V^r_k	relative selectivity of research divers for paua in the *k*th length class
V^s_k	relative selectivity of commercial divers for paua in the *k*th length class
$\sigma^r_{k,t}$	error of the predicted proportion in the k^{th} length class in year *t* in RDLF data
n^r_t	relative weight (effective sample size) of the RDLF data in year *t*
$\sigma^s_{k,t}$	error of the predicted proportion in the k^{t}h length class in year *t* in CSLF data
n^s_t	relative weight (effective sample size)of the CSLF data in year *t*
σ^d_j	standard deviation of the predicted length increment for the j^{th} tag-recapture record
σ^{tag}_j	total error predicted for the j^{th} tag-recapture record
σ^{mat}_k	error of the proportion mature-at-length for the k^{th} length class
$-\ln(\mathbf{L})$	negative log-likelihood
f	total function value

2.2.5 Predictions

$\hat{I}_t$	predicted CPUE in year *t*
$\hat{I}2_t$	predicted PCPUE in year *t*
$\hat{J}_t$	predicted RDSI in year *t*
$\hat{p}^r_{k,t}$	predicted proportion in the k^{th} length class in year *t* in research diver surveys
$\hat{p}^s_{k,t}$	predicted proportion in the k^{th} length class in year *t* in commercial catch sampling
$\hat{d}_j$	predicted length increment of the j^{th} tag-recapture record
$\hat{p}^{mat}_k$	predicted proportion mature in the k^{th} length class

2.2.6 Initial conditions

The initial population is assumed to be in equilibrium with zero fishing mortality and the base recruitment. The model is run for 60 years with no fishing to obtain near-equilibrium in numbers-at-length. Recruitment is evenly divided among the first five length bins:

(1) $R_{k,t} = 0.2R0$ for $1 \le k \le 5$

(2) $R_{k,t} = 0$ for $k > 5$

A growth transition matrix is calculated inside the model from the estimated growth parameters. If the growth model is linear, the expected annual growth increment for the *k*th length class is

$$\Delta l_k = \left(\frac{\beta g_\alpha - \alpha g_\beta}{g_\alpha - g_\beta} - l_k \right) \left[1 - \left(1 + \frac{g_\alpha - g_\beta}{\alpha - \beta} \right) \right] \quad (3)$$

The model uses the AD Model Builder™ function *posfun*, with a dummy penalty, to ensure a positive expected increment at all lengths, using a smooth differentiable function. The *posfun* function is also used with a real penalty to force the quantity $\left(1 + \frac{g_\alpha - g_\beta}{\alpha - \beta} \right)$ to remain positive. If the growth model is exponential (used for the base case), the expected annual growth increment for the *k*th length class is

$$\Delta l_k = g_\alpha \left(g_\beta / g_\alpha \right)^{(l_k - \alpha)/(\beta - \alpha)} \quad (4)$$

again using *posfun* with a dummy penalty to ensure a positive expected increment at all lengths.

The standard deviation of g_k is assumed to be proportional to g_k with minimum σ_{MIN}:

$$\sigma^{g_k} = \left(g_k \phi - \sigma_{MIN} \right) \left(\frac{1}{\pi} \tan^{-1} \left(10^6 \left(g_k \phi - \sigma_{MIN} \right) \right) + 0.5 \right) + \sigma_{MIN} \quad (5)$$

From the expected increment and standard deviation for each length class, the probability distribution of growth increments for a paua of length l_k is calculated from the normal distribution and translated into the vector of probabilities of transition from the k^{th} length bin to other length bins to form the growth transition matrix **G**. Zero and negative growth increments are permitted, i.e., the probability of staying in the same bin or moving to a smaller bin can be non-zero.

In the initialisation, the vector $\mathbf{N_t}$ of numbers-at-length is determined from numbers in the previous year, survival from natural mortality, the growth transition matrix **G,** and the vector of recruitment $\mathbf{R_t}$:

$$\mathbf{N_t} = \left(\mathbf{N_{t\text{-}1}} \, e^{-M} \right) \bullet \mathbf{G} + \mathbf{R_t} \quad (6)$$

where the dot (•) denotes matrix multiplication.

2.2.7 Dynamics

2.2.7.1 Sequence of operations

After initialising, the first model year is 1965 and the model is run through to 2009. In the first 9 years the model is run with an assumed catch vector, because it is unrealistic to assume that the fishery was in a virgin state when the first catch data became available in 1974. The assumed catch vector rises linearly from zero to the 1974 catch. These years can be thought of as an additional part of the initialisation, but they use the dynamics described in this section.

Model dynamics are sequenced as follows.

- Numbers at the beginning of year *t*-1 are subjected to fishing, then natural mortality, then growth to produce the numbers at the beginning of year *t*.

- Recruitment is added to the numbers at the beginning of year *t*.

- Biomass available to the fishery is calculated and, with catch, is used to calculate the exploitation rate, which is constrained if necessary.

- Half the exploitation rate (but no natural mortality) is applied to obtain mid-season numbers, from which the predicted abundance indices and proportions-at-length are calculated. Mid-season numbers are not used further.

2.2.7.2 Main dynamics

For each year *t*, the model calculates the start-of-the-year biomass available to the commercial fishery. Biomass available to the commercial fishery is:

$$B_t = \sum_k N_{k,t} V_k^s w_k \tag{7}$$

$$V_k^{t,s} = \frac{1}{1+19^{-\left((l_k - D_{50})/D_{95-50}\right)}} \quad \text{for } t < 2007 \tag{8}$$

$$V_k^{t,s} = \frac{1}{1+19^{-\left((l_k - D_{50} - 5)/D_{95-50}\right)}} \quad \text{for } t \geq 2007 \tag{9}$$

The observed catch is then used to calculate exploitation rate, constrained for all values above U^{max} with the *posfun* function of AD Model Builder™. If the ratio of catch to available biomass exceeds U^{max}, then exploitation rate is constrained and a penalty is added to the total negative log-likelihood function. Let minimum survival rate A_{min} be 1-U^{max} and survival rate A_t be 1-U_t:

$$A_t = 1 - \frac{C_t}{B_t} \quad \text{for } \frac{C_t}{B_t} \leq U^{\max} \tag{10}$$

$$A_t = 0.5 A_{\min}\left[1 + \left(3 - \frac{2\left(1 - \frac{C_t}{B_t}\right)}{A_{\min}}\right)^{-1}\right] \quad \text{for } \frac{C_t}{B_t} > U^{\max} \tag{11}$$

The penalty invoked when the exploitation rate exceeds U^{max} is:

$$1000000\left(A_{\min} - \left(1 - \frac{C_t}{B_t}\right)\right)^2 \tag{12}$$

This prevents the model from exploring parameter combinations that give unrealistically high exploitation rates. Survival from fishing is calculated as:

(13) $SF_{k,t} = 1 - (1 - A_t) P_{k,t}$

or

(14) $SF_{k,t} = 1 - (1 - A_t) V_k^s$

The vector of numbers-at-length in year *t* is calculated from numbers in the previous year:

(15) $\mathbf{N_t} = \left(\left(\mathbf{SF_{t-1}} \otimes \mathbf{N_{t-1}} \right) \mathrm{e}^{-M} \right) \bullet \mathbf{G} + \mathbf{R_t}$

where $\otimes$ denotes the element-by-element vector product. The vector of recruitment, $\mathbf{R_t}$, is determined from *R0* and the estimated recruitment deviations:

(16) $R_{k,t} = 0.2 R0 e^{\left(\varepsilon_t - 0.5 \sigma_\varepsilon^2 \right)}$ for $1 \le k \le 5$

(17) $R_{k,t} = 0$ for $k > 5$

The recruitment deviation parameters ε_t were estimated for all years from 1977; there was no constraint for deviations to have a mean of 1 in arithmetic space except for the constraint of the prior, which had a mean of zero in log space; and we assumed no stock recruitment relationship.

2.2.8 Model predictions

The model predicts CPUE in year *t* from mid-season recruited biomass, the scaling coefficient, and the shape parameter:

(18) $\hat{I}_t = q^I \left(B_{t+0.5} \right)^h$

Available biomass $B_{t+0.5}$ is the mid-season vulnerable biomass after half the catch has been removed (no natural mortality is applied, because the time over which half the catch is removed might be short). It is calculated as in equation (7), but using the mid-year numbers, $N_{k,t+0.5}$:

(19) $N_{k,t+0.5}^{vuln} = N_{k,t} \left(1 - \frac{(1 - A_t)}{2} V_k^s \right).$

Similarly,

(20) $\hat{I}2_t = q^{I2} \left(B_{t+0.5} \right)^h = X q^I \left(B_{t+0.5} \right)^h$

The same shape parameter *h* is used for both series: experiment outside the model showed that this was appropriate despite the different units of measurement for the two series. The predicted research diver survey index is calculated from mid-season model numbers in bins greater than 89 mm length, taking into account research diver selectivity-at-length:

(21) $N_{k,t+0.5}^{res} = N_{k,t} \left(1 - \frac{(1 - A_t)}{2} V_k^r \right)$

(22) $$\hat{J}_t = q^J \sum_{k=11}^{55} N_{k,t+0.5}^{res}$$

where the scalar is estimated and the research diver selectivity V_k^r is calculated from:

(23) $$V_k^r = \frac{1}{1+19^{-\left((l_k - T_{50})/T_{95-50}\right)}}$$

The model predicts proportions-at-length for the RDLF from numbers in each length class for lengths greater than 89 mm:

(24) $$\hat{p}_{k,t}^r = \frac{N_{k,t+0.5}^{res}}{\sum_{k=11}^{51} N_{k,t+0.5}^{res}} \qquad \text{for } 11 \le k < 51$$

Predicted proportions-at-length for CSLF are similar:

(25) $$\hat{p}_{k,t}^s = \frac{N_{k,t+0.5}^{vuln}}{\sum_{k=23}^{51} N_{k,t+0.5}^{vuln}} \qquad \text{for } 23 \le k < 51$$

The predicted increment for the *j*th tag-recapture record, using the linear model, is

(26) $$\hat{d}_j = \left(\frac{\beta g_\alpha - \alpha g_\beta}{g_\alpha - g_\beta} - L_j \right) \left[1 - \left(1 + \frac{g_\alpha - g_\beta}{\alpha - \beta} \right)^{\Delta t_j} \right]$$

where Δt_j is in years. For the exponential model (used in the base case) the expected increment is

(27) $$\hat{d}_j = \Delta t_j g_\alpha \left(g_\beta / g_\alpha \right)^{(L_j - \alpha)/(\beta - \alpha)}$$

The error around an expected increment is

(28) $$\sigma_j^{\,d} = \left(\hat{d}_j \phi - \sigma_{MIN} \right) \left(\frac{1}{\pi} \tan^{-1} \left(10^6 \left(\hat{d}_j \phi - \sigma_{MIN} \right) \right) + 0.5 \right) + \sigma_{MIN}$$

Predicted maturity-at-length is

(29) $$\hat{p}_k^{mat} = \frac{1}{1+19^{-\left((l_k - L_{50})/L_{95-50}\right)}}$$

2.2.9 Fitting

2.2.9.1 Likelihoods

The distribution of CPUE is assumed to be normal-log and the negative log-likelihood is:

$$-\ln(\mathbf{L})\left(\hat{I}_t \mid \theta\right) = \frac{\left(\ln\left(I_t\right) - \ln\left(\hat{I}_t\right)\right)^2}{2\left(\sigma_t^I \Big/ \varpi^I\right)^2} + \ln\left(\sigma_t^I \Big/ \varpi^I\right) + 0.5\ln\left(2\pi\right) \tag{30}$$

and similarly for PCPUE:

$$-\ln(\mathbf{L})\left(\hat{I}2_t \mid \theta\right) = \frac{\left(\ln\left(I2_t\right) - \ln\left(\hat{I}2_t\right)\right)^2}{2\left(\sigma_t^{I2} \Big/ \varpi^{I2}\right)^2} + \ln\left(\sigma_t^{I2} \Big/ \varpi^{I2}\right) + 0.5\ln\left(2\pi\right) \tag{31}$$

The distribution of the RDSI is also assumed to be normal-log and the negative log-likelihood is:

$$-\ln(\mathbf{L})\left(\hat{J}_t \mid \theta\right) = \frac{\left(\ln\left(J_t\right) - \ln\left(\hat{J}_t\right)\right)^2}{2\left(\sigma_t^J \Big/ \varpi^J\right)^2} + \ln\left(\sigma_t^J \Big/ \varpi^J\right) + 0.5\ln\left(2\pi\right) \tag{32}$$

The proportions-at-length from CSLF data are assumed to follow a multinomial distribution, with a standard deviation that depends on the effective sample size (see section 2.2.9.3) and the weight assigned to the data:

$$\sigma_{k,t}^s = \frac{\tilde{\sigma}}{\varpi^s n_t^s} \tag{33}$$

The negative log-likelihood is:

$$-\ln(\mathrm{L})\left(\hat{p}_{k,t}^s \mid \theta\right) = \frac{p_{s,t}^s}{\sigma_{k,t}^s}\left(\ln\left(p_{k,t}^s + 0.01\right) - \ln\left(\hat{p}_{k,t}^s + 0.01\right)\right) \tag{34}$$

The likelihood for research diver sampling is analogous. Errors in the tag-recapture dataset were also assumed to be normal. For the *j*th record, the total error is a function of the predicted standard deviation (equation (28)), observation error, and weight assigned to the data:

$$\sigma_j^{tag} = \varpi^{tag}\sqrt{{\sigma_{obs}}^2 + \left(\sigma_j^{\,d}\right)^2} \tag{35}$$

and the negative log-likelihood is:

(36) $$-\ln(\mathbf{L})\left(\hat{d}_j \mid \theta\right) = \frac{\left(d_j - \hat{d}_j\right)^2}{2\left(\sigma_j^{tag}\right)^2} + \ln\left(\sigma_j^{tag}\right) + 0.5\ln\left(2\pi\right)$$

The proportion mature-at-length was assumed to be normally distributed, with standard deviation analogous to proportions-at-length:

(37) $$\sigma_k^{mat} = \frac{\%}{\varpi^{mat}\sqrt{p_k^{mat} + 0.1}}$$

The negative log-likelihood is:

(38) $$-\ln(\mathbf{L})\left(\hat{p}_k^{mat} \mid \theta\right) = \frac{\left(p_k^{mat} - \hat{p}_k^{mat}\right)^2}{2\left(\sigma_k^{mat}\right)^2} + \ln\left(\sigma_k^{mat}\right) + 0.5\ln\left(2\pi\right)$$

2.2.9.2 Normalised residuals

These are calculated as the residual divided by the relevant σ term used in the likelihood. For CPUE, the normalised residual is

(39) $$\frac{\ln\left(I_t\right) - \ln\left(\hat{I}_t\right)}{\left(\sigma_t^I \,/\, \varpi^I\right)}$$

and similarly for PCPUE and RDSI. For the CSLF proportions-at-length, the residual is

(40) $$\frac{p_{k,t}^s - \hat{p}_{k,t}^s}{\sigma_{k,t}^s}$$

and similarly for proportions-at-length from the RDLFs. Because the vectors of observed proportions contain many empty bins, the residuals for proportions-at-length include large numbers of small residuals, which distort the frequency distribution of residuals. When presenting normalised residuals from proportions-at-length, we arbitrarily ignore normalised residuals less than 0.05.

For tag-recapture data, the residual is

(41) $$\frac{d_j - \hat{d}_j}{\sigma_j^{tag}}$$

and for the maturity-at-length data the residual is

(42) $$\frac{p_k^{mat} - \hat{p}_k^{mat}}{\sigma_k^{mat}}$$

2.2.9.3 Dataset weights

Weights were chosen experimentally for each dataset, iteratively changing them to obtain standard deviations of the normalised residuals (*sdnr*) close to unity for each dataset.

Proportions at length (CSLF and RDLF) were included in the model with a multinomial likelihood. The length frequencies for individual years were assigned relative weights (effective sample sizes), based on a sample size that represented the best least squares fit of $\log(cv_i)$~$\log(P_i)$, where cv_i was the bootstrap c.v. for the ith proportion, P_i. Estimated and actual sample sizes for the commercial catch and research diver proportions at length for are given in Table 1Table 2. (See also Appendix A, Figures A1 & A2 for a plot of the relationship). The weights for individual years were further adjusted by the weight assigned to the dataset in the model.

2.2.9.4 Priors and bounds

Bayesian priors were established for all estimated parameters (Table 3). Most were incorporated simply as uniform distributions with upper and lower bounds arbitrarily set wide so as not to constrain the estimation. The prior probability density for M was a normal-log distribution with mean μ_M and standard deviation σ_M . The contribution to the objective function of estimated $M = x$ is:

$$-\ln(\mathbf{L})(x \mid \mu_M, \sigma_M) = \frac{\left(\ln(M) - \ln(\mu_M)\right)^2}{2\sigma_M{}^2} + \ln\left(\sigma_M \sqrt{2\pi}\right) \tag{43}$$

The prior probability density for the vector of estimated recruitment deviations, ε , was assumed to be normal with a mean of zero and a standard deviation of 0.4. The contribution to the objective function for the whole vector is:

$$-\ln(\mathbf{L})(\varepsilon \mid \mu_\varepsilon, \sigma_\varepsilon) = \frac{\sum_{i=1}^{n_\varepsilon} (\varepsilon_i)^2}{2\sigma_\varepsilon{}^2} + \ln\left(\sigma_\varepsilon\right) + 0.5\ln(2\pi). \tag{44}$$

Constant parameters are given in Table 4.

2.2.9.5 Penalty

A penalty is applied to exploitation rates higher than the assumed maximum (equation 12); it is added to the objective function after being multiplied by an arbitrary weight (1E6) determined by experiment.

AD Model Builder™ also has internal penalties that keep estimated parameters within their specified bounds, but these should have no effect on the final outcome, because choice of a base case excludes the situations where parameters are estimated at or near a bound.

2.2.10 Fishery indicators

The assessment reports the following indicators calculated from their posterior distributions: the model's mid-season spawning and recruited biomass for 2009 ($B_{current}$ and $B^r_{current}$), for 2012 (B_{2012} and B^r_{2012}), and from the nadir (lowest point) of the population trajectory ($B_{\min}$ and $B^r_{\min}$).

The assessment reports B_{init} — the spawning stock biomass at the end of initialisation phase (the equilibrium biomass assuming recruitment being equal to base recruitment and no fishing), and B_0 — the equilibrium spawning stock biomass assuming recruitment being equal to the average recruitment from the period for which recruitment deviation were estimated. B_0 will differ from B_{init} if estimated average recruitment deviates from base recruitment (this will generally be true because the model has no constraint on the recruitment deviations aside from the priors). The ratio of $B_{current}$ to B_0 is a preferred indicator of current stock status (B_{init} was considered to bear little biological meaning). The assessment also reports $B^r_{current}$, B^r_{init}, and B^r_0, being the current, initial, and virgin recruit-sized biomass respectively.

2.2.11 Markov chain-Monte Carlo (MCMC) procedures

AD Model Builder™ uses the Metropolis-Hastings algorithm. The step size is based on the standard errors of the parameters and their covariance relationships, estimated from the Hessian matrix.

For the MCMCs in this assessment we ran single long chains that started at the MPD estimate. The base case was 5 million simulations long and we saved samples, regularly spaced by 5000. We fixed the value of σ_R to that used in the MPD run because it may be inappropriate to let a variance component change during the MCMC.

2.2.12 Base case and sensitivity model runs

Following Working Group discussions, a base case (referred to as model 1.0) has been chosen for this assessment. The base case used model specifications as described above, and included:

- a catch vector estimated under the base case assumption (40% of the commercial catch in Statistical Area 030 was taken from PAU 5A annually between 1985 and1996)
- a standardised CPUE series based on CELR data from Statistical Area 030 for 1990–2001
- a standardised CPUE series based on PCELR data for 2002–2009
- a standardised research diver survey index for 1996, 2002, 2003, 2006, 2008, and 2009
- a research diver survey proportions-at-lengths series for 1996, 2002, 2003, 2006, and 2009
- a commercial catch sampling length frequency series for 2002–2005
- tag-recapture length increment data
- maturity-at-length data.

The exponential growth model was used to fit the tag-recapture (other growth models were explored but not adopted). Recruitment deviations were estimated for 1986–2006. The relative weights for each dataset were adjusted iteratively until the standard deviations of the normalised residuals were close to 1.0 for each dataset (referred to as natural weights).

Sensitivity trials were conducted for the MPD fits, based on variations to the base case: model 1.1 up-weighted the CPUE dataset; model 1.2 estimated recruitment deviations for 1992–2006; model 2.0

included additional years of CSLF and model 3.0 removed all CSLF data; models 4.0 and 5.0 used alternative catch estimates made under the upper-bound and lower-bound assumptions respectively (61% or 18% of the commercial catch in Statistical Area 030 was taken from PAU 5A annually between 1985 and1996); model 5.1 is based on model 5.0 but up-weighted the CPUE dataset. A summary of model descriptions for the base case and sensitivity trials are given in Table 5. MCMC simulations were conducted for the base case, and only MPD results were given for the sensitivity trials.

3. RESULTS

3.1 MPD base case

Model estimates of objective function values (negative log-likelihood), parameters, and indicators for the base case are given in the second column of Table 6.

The base case model fits the two observed CPUE abundance indices credibly (Figure 2-top and middle); though it is unable to fit the initial decline in the CPUE indices between 1990 and 1994. The fits to the RDSI are poor (Figure 2-bottom): the model is unable to explain the inter-annual changes in the observed RDSI, although it suggests a similar declining trend overall.

Fits to commercial proportions-at-length are reasonably good (Figure 3) and there is no consistent pattern between the residuals and length (Figure 5). Fits to research diver proportions-at-length are less adequate (**Error! Reference source not found.**), particularly for the 2002 and 2003 samples where the model has missed the mode of the length distribution, and overestimated the proportions of large paua (over 140 mm, Figure 6).

The QQ plots of the residuals show no apparent departure from the normal assumption (Figure 7). The weights chosen gave standard deviations of normalised residuals that were very close to 1 for all data sets (see Table 6). The standard deviations associated with the data encompassed the observational error, the common error term ($\tilde{\sigma}$), and the weight (see Section 2.9.11). For the CPUE data the resulting standard deviations are 25% more than the observational error; for the RDLF data they are 40% less. The total errors for PCPUE, CSLF and RDSI data are close to their observational error, with little or no process errors added.

The MPD estimate of M was 0.12, close to the assumed mean of the prior distribution, 0.10. Estimates of maturity ogives were sensible, with length at 50% and full maturity estimated to be approximately 92 and 110 mm (Figure 8). Estimates of growth parameters suggested a mean annual growth of 23 mm at 75 mm and 7.4 mm at 120 mm, with a c.v. of about 0.30. The estimated growth transition matrix appeared to have accounted for most of the variability in the growth data (Figure 9).

The midpoint of the research diver selectivity ogive was 107.9 mm, and the ogive was broad as in previous assessments (Figure 10). The midpoint of the commercial fishery selectivity was 126.3 mm, just slightly above the MLS, and this ogive was very narrow (Figure 10).

The model's MPD estimates of recruitment were lower than average in the late 1980 and about average through the 1990s (**Error! Reference source not found.**).

The MPD estimates for the spawning stock biomass (mature animals) and recruited biomass (animals at or above the MLS) are shown in Figure 12. Both recruited and spawning biomass decreased substantially from the 1965, but have shown slight increases over the last few years. $B_{current}$ is estimated to be about 35% of B_0, and $B^r_{current}$ is estimated to be about 23% of B^r_0 (Figure 13)

3.2 MPD sensitivity trials

Model estimates of objective function values (negative log-likelihood), parameters, and indicators for sensitivity trials are given in Table 6. Selected model fits are shown in Figures A3–A9, Appendix A. For each of the models the weights were chosen to give standard deviations of normalised residuals that were very close to 1 for all data sets (see Table 6), except for models 1.1 and 5.1 in which the CPUE data was up-weighted (see below).

For model run 1.1, an arbitrary but large weight of 4.0 was assigned to the CPUE data whereas weights for other datasets were fixed at the base case values. The up-weighting had the effect of halving the standard deviation of the observed CPUE data. The fit to the CPUE indices was improved, particularly for the early part of the series (see Figure A3). The SDNR of the fits increased to 1.4, suggesting some level of over-fitting. The estimated biomass trajectory is similar to the base case, except for a slightly steeper decline between the late 1980s and early 1990, possibly driven by changes in the estimated recruitment deviations (Figure 14). $B_{current}$ is estimated to be about 32% of B_0. There were little changes in the fits to other datasets (see Figure A3).

For model run 1.2, recruitment deviation was estimated for 1992–2006, five years less than the base case. The fits to the CPUE appears to be slightly worse (see Figure A4), which is to be expected given that fewer free parameters were available. Model fits to other datasets and estimated biomass trajectory are similar to the base case, with $B_{current}$ estimated to be about 33% of B_0.(see Figure 14).

Model run 2.0 includes additional CSLF data (1992–94, 1998, 2001, and 2006–09). The model virtually can not fit the CPUE, and the fits to the new CSLF are generally not satisfactory (Figure A5). The estimated biomass trajectory showed an opposite trend between mid 1980s to mid 1990s to the base case (Figure 15–top), and the estimated recruitment deviations were markedly different (Figure 15–bottom; note that five additional years of recruitment deviations were estimated due to inclusion of new CSLF data). This suggested there could be some conflicts between datasets (see later in this section). Model run 3.0 has removed the CSLF data, with commercial fishing selectivity fixed at the base case estimates. The biomass estimates were similar to the base case (see Figure 15), but predicted commercial catch length frequencies deviated from the observed length frequencies for most years (Figure A6). There were also some changes to the estimated recruitment deviations when the CSLF data were excluded (see Figure 15–bottom).

Alternative estimates of catch history were investigated. Model run 4.0 was based on the upper bound assumption (61% of the annual commercial catch in Statistical Area 030 was taken from PAU 5A between 1984 and 1996). The fits to most datasets were similar to the base case, but the fits to the CPUE were slightly better (Figure A7). When the catch vector estimated under the lower bound assumption (18%) was used, the model was unable to fit the CPUE (Model run 5.0, see Figure A8), unless a large weight was assigned to the CPUE dataset (Model run 5.1, see Figure A9). Estimates of biomass trajectory were different under those assumptions, mainly for the early years (Figure 16), with $B_{current}$ ranging from 30% to 52% of B_0.

In general, model estimates of biological parameters for sensitivity trials were similar to the base case, but estimates of stock status were sensitive to the assumed catch history, with B_{current} ranging from 30 to 52% of B_0, and $B^r_{current}$ ranging from 23 to 43% of B^r_0. Fits to the PCPUE, CSLF, and RDLF were similar for most model runs. Models with higher catch estimates appeared to fit the CPUE better, but none of the models were able to improve the fits to the RDSI.

The profile likelihood on R_0 was investigated, based on model run 2.0 (This is the model showing potential conflicts of the data.). Changes of objective function value (both the total and the component likelihood) for a range of R_0 in relation to their MPD estimates are shown in Figure 17. A minor modification was made where a penalty function was imposed to encourage the average recruitment deviation to be close to 1 (otherwise, the changes of R_0 will be offset by changes in recruitment

deviations without much impact on model fits). Within the range of R_0 considered the total likelihood changed about 40 units, mostly driven by changes in the fits to the length frequency data and the prior of *M*. The conflict between the CSLF and the CPUE is also apparent.

3.3 MCMC results

MCMC simulations were conducted for the base case. The main diagnostic we used for the MCMC is the trace and autocorrelation plots for the posterior samples (Figure 18). The MCMC traces showed good mixing and there is no excessive autocorrelation within the sampled chain for all the estimated parameters and indicators. In general there is no obvious evidence that the chain is not converged. The MCMC parameter correlation matrix (Table 7) shows a high correlation between recruitment and *M*, as is usually seen; between the c.v. of growth and the other two growth parameters; between the two research diver selectivities; the two commercial selectivity parameters; and between the abundance scalars and one of the growth parameters. This list does not seem excessive.

3.4 Marginal posterior distributions and the Bayesian fit

Posteriors (**Error! Reference source not found.**) for all estimated parameter and indicators were generally well formed and MPDs were mostly near the centres (but tended to be below the median of biomass posteriors). Posteriors of the sdnrs were mostly in the range from 0.8 to 1.2. The posteriors are summarised Table 8in Table 8.

The posteriors of fits to CPUE and to PCPCE appear to be adequate, although in some years have predictions that do not encompass the observed values (Figure 19). The posteriors of fits to RDSI (Figure 19) were poor. In contrast with the observed RDSI, the predicted RDSI show only a slightly declining trend. The model also seems unable to reproduce the range of variation seen in the RDSI data.

The posteriors of fits to CSLFs were very reasonable, except that they did not match the observed values for the peak size bins just above the MLS for 2002 and 2003 (Figure 20). The posteriors of fits to RDLF were poor for 2001, 2003, and 2006, but were acceptable for other years (Figure 21).

The posteriors of selectivities are tight (Figure 22). Median recruitment is also similar to the MPD, but individual estimates show some level of uncertainty (Figure 23). Exploitation rate was generally below 0.4 but was variable (Figure 24). The exploitation rate has been high since the late 1990s, but showed decreases over the last few years, in line with the reduction of catch levels.

The posterior trajectory of spawning stock biomass is shown in Figure 25, of recruited biomass in Figure 26, and the posterior trajectory of spawning stock depletion is shown in Figure 27.

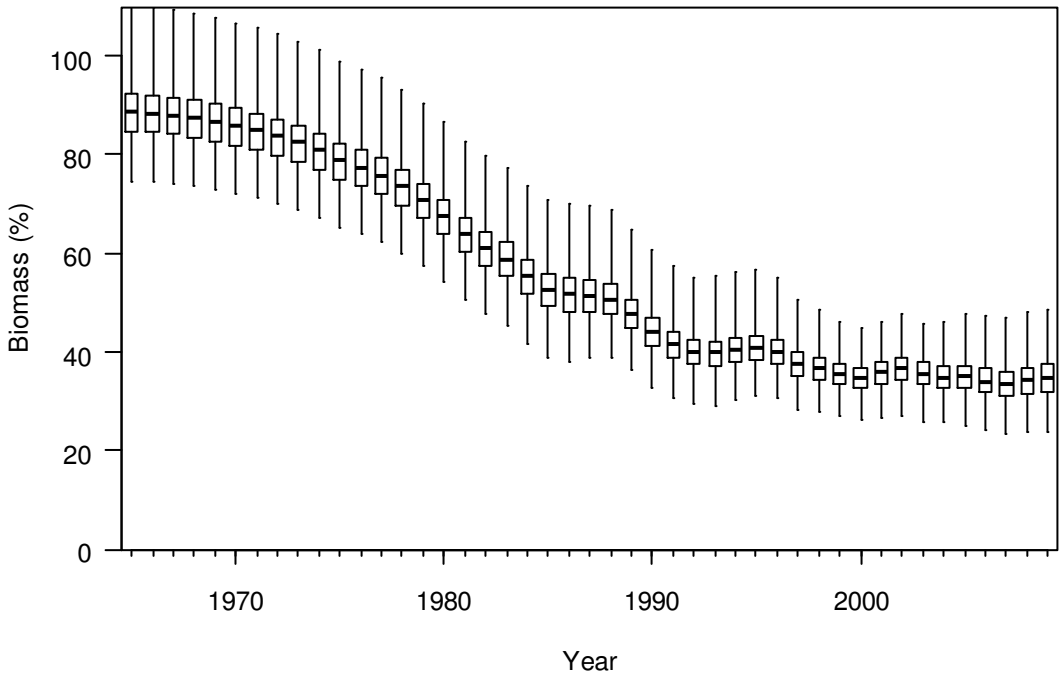

Figure 25. Posterior trajectory of spawning stock biomass.

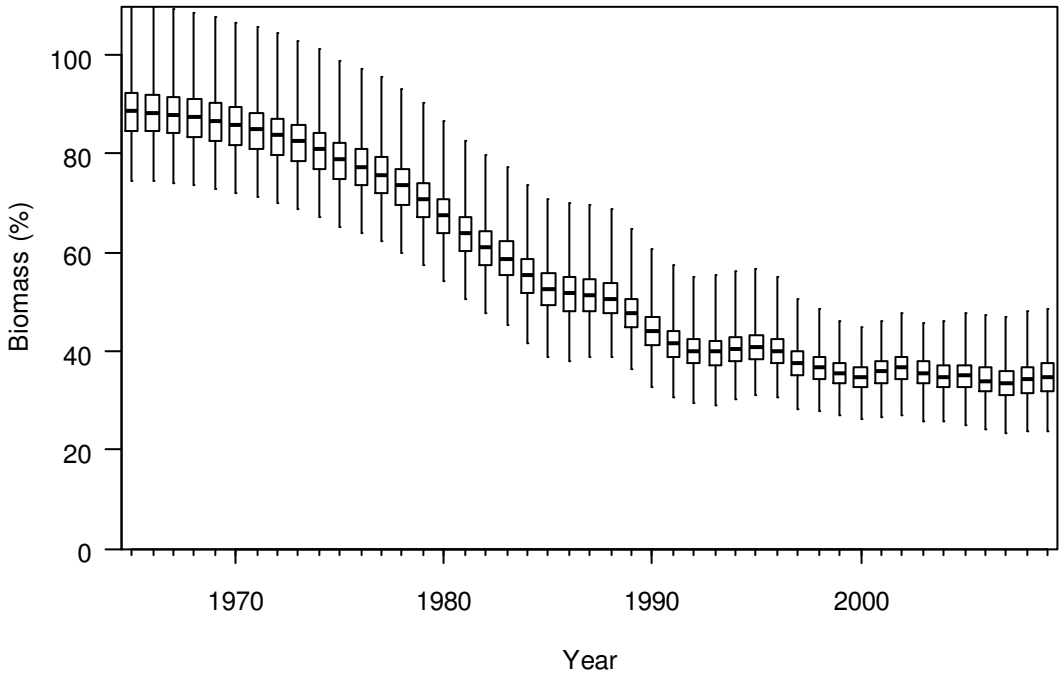

Figure 26. Posterior trajectory of recruited biomass.

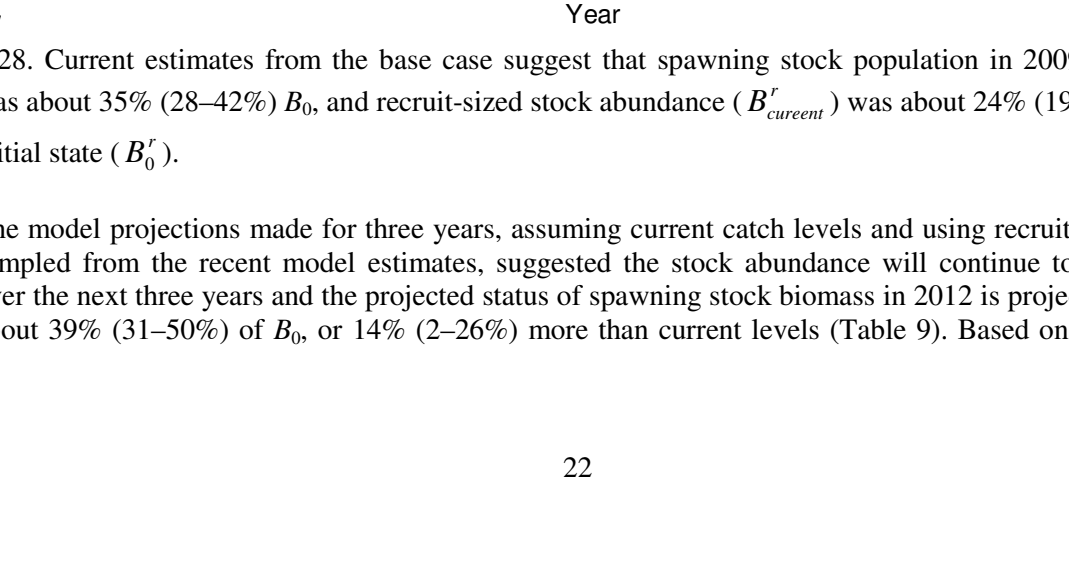

Figure 27. Posterior trajectory of spawning stock depletion.

Current estimates from the base case suggest that spawning stock population in 2009 (B_{current}) was about 35% (28–42%) B_0, and recruit-sized stock abundance ($B^r_{cureent}$) was about 24% (19–29%) of initial state (B^r_0).

The model projections made for three years, assuming current catch levels and using recruitments re-sampled from the recent model estimates, suggested the stock abundance will continue to increase over the next three years and the projected status of spawning stock biomass in 2012 is projected to be about 39% (31–50%) of B_0, or 14% (2–26%) more than current levels (Table 9). Based on the 1000

posterior samples, the probability for the spawning stock biomass to decrease in three year's time is less than 7%.

4. DISCUSSION

Assessments for New Zealand paua stocks have previously been conducted at the Quota Management Area level, as the fishery management measures are usually made at such scales. For PAU 5A, there were concerns about the applicability of the assessment to the entire QMA, although there was general agreement that biomass decline had occurred in the southern region of the QMA over recent years. If abundances changes have differed between subareas, a QMA-level model assuming a homogeneus area is unlikely to be informative regarding the stock status.

There have been changes in management initiatives in recent years towards fine-scale management of paua stocks. Subarea management zones, based on the research strata, have been established in PAU 5A since 2006, with voluntary catch limit and minimum harvest size in place for each zone. Therefore a subarea level assessment is probably more relevant in informing management decisions. In addition, improvement of the collection and reporting of fishery data at finer scale has allowed the development of models to assess the fish stock at smaller spatial scale.

This report assesses the southern subarea of PAU 5A (Chalky and South Coast). Although the choice of areas to be assessed was made tentatively based on availability of data, this could serve as a stepping-stone towards more fine-scale assessment in the future, in line with the refinement of data collection and the establishment of finer scale fishery management.

Estimates from the base case model suggested that current spawning stock population (B_{current}) was 35% (28–42%) B_0, and recruit-sized stock abundance ($B^r_{current}$) was 24% (19–29%) of initial state (B^r_0). The model projections made for three years assuming current catch levels and using recruitments re-sampled from the recent model estimates suggested the stock abundance will continue to increase over the next three years, and the projected status of spawning stock biomass in 2012 is 39% (31–50%) of B_0.

The model presented here, whilst fairly representing some of the data, also shows some indications of lack of fit. It is unlikely the estimates of historical stock size are reliable, given assumptions about annual recruitment and the use of the historical catch-effort indices of abundance. However, model estimates of recent status generally agree closely with recent CPUE trends.

We made no attempt to compare the results from this study with the previous assessment for several reasons, apart from the fact that a smaller area is covered in this assessment. Firstly, the revised catch history for PAU 5A is considerably different from previous assessment. Secondly, separate CPUE and PCPUE indices are used whereas a combined CELR/PCELR were used previously. Thirdly, the method for calculating research diver survey indices has been revised slightly. Fourthly, only four years of commercial catch sampling series are included. However, we noticed that estimates of biological parameter estimates (maturity, growth, and mortality) are very similar for both assessments.

Although the assessment is conducted at a smaller spatial scale, the model treats the whole of the assessed southern strata of PAU 5A as if it were a single stock with homogeneous biology, habitat, and fishing pressures. This means the model assumes homogeneity in recruitment, that natural mortality does not vary by size or year, and that growth has the same mean and variance throughout the area (paua fisheries are extremely variable and paua populations can change in very short distances along the coast). Heterogeneity in growth can be a problem for this kind of model (Punt 2003). Variation in growth is addressed to some extent by having a stochastic growth transition matrix based on increments observed in several different places; similarly the length frequency data are integrated across samples from many places.

The effect is likely to make model results optimistic. For instance, if some local stocks are fished very hard and others not fished, recruitment failure can result because of the depletion of spawners, because spawners must breed close to each other and because the dispersal of larvae is unknown and may be limited. Recruitment failure is a common observation in overseas abalone fisheries, local processes may decrease recruitment, which is an effect that the current model cannot account for. Another concern is that the model could overestimate productivity in the population as a whole if fishing has caused spatial contraction of populations (e.g., Shepherd & Partington 1995) if some populations become relatively unproductive after initial fishing (Gorfine & Dixon 2000).

The commercial catch before 1974 is unknown and, although we think the effect is minor, major differences may exist between the catches we assume and what was taken. In addition, non-commercial catch estimates are poorly determined and could be substantially different from what was assumed, with illegal catch particularly suspect.

There were uncertainties in the estimated catch history relating to the division of the pre-QMA catch among the three substocks of PAU 5 and between subareas within PAU 5A. Sensitivity trials have used catch estimates made under alternative assumptions. Between the lower-bound and upper-bound catch estimates, model estimates of current spawning stock status ranged from 30 to 52% of B_0. There is little information on the historic catches in Fiordland, but anecdotal evidence suggested the catch between 1981 and 1984 were about 60-70 tonne annually (Storm Stanley pers. comm.). This suggested that the lower bound estimates are too low, and the upper bound estimates are too high. The general consensus is that there had been a redistribution of catch when the quota was split among the substocks but the extent to which this happened is unknown. However, the lower and upper bound estimates should have encompassed many of the uncertainties in the historic catches.

CPUE provides information on changes of relative abundance. However, CPUE is generally considered to be a poor index of stock abundance for paua, due to divers' ability to maintain catch rates by moving from area to area despite a decreasing biomass (hyperstability). Breen et al. (2003) argued standardised CPUE might be able to relate to the changes of abundance in a fully exploited fishery, and a large decline in the CPUE is most likely to reflect a decline in the fishery. However, for the southern area of PAU 5A, the interpretation of the decline of CPUE in the early 1990s is confounded by the shifting of fishing effort from Stewart Island to South Coast (the CPUE is based on Statistical Area 030). The fishers suggested the catch rates had declined markedly in Stewart Island during this period, but to what extent the CPUE reflected abundance in Chalky and South Coast is unknown. Attempts to estimate the relationship between CPUE and biomass (through the parameter h) have been made in some of the previous paua stock assessments and on some occasions have suggested evidence of hyperstability (McKenzie 2009). In this study estimation of parameter h has been unsuccessful.

Commercial catch length frequencies provide information on changes in population structure under fishing pressure. However, if serial depletion had occurred and fishers had moved from area to area, samples from the commercial catch may have represented the population of the entire stock. For Chalky and South Coast, only four years of catch sampling (2002–05) were considered to be adequate, and the sampling coverage is low since then and dubious before then. It is anticipated that the sampling coverage will be improved in the future.

The research diver survey indices exhibited large inter-annual variations and were fitted poorly in all model runs. The usefulness of research diver survey indices in providing relative abundance information has been an ongoing concern. Cordue (2009) concluded that the diver survey based on the timed swim approach is fundamentally flawed and is inadequate for providing relative abundance indices. A current review of survey methodology is underway and the preliminary results suggest that the existing RDSI data are likely to be more useful at stratum level. The general consensus is the index-abundance relationship from the research diver survey is likely to be nonlinear, and can not be easily quantified in a stock assessment.

Model fits to the length frequencies from the research diver survey were acceptable, though structures were apparent in some years. Cordue (2009) suggested that RDLF are probably more useful at individual stratum level. The RDLF combined across strata may not be able to represent the underlying population at larger scale as the weight of individual strata can not be determined.

The growth was estimated from combined tag-recapture and isotopic increment data using an integrated approach. Model fits to growth data appeared adequate. However, it is unknown how accurate the growth estimates are. The data may not reflect fully the average growth and range of growth in this population. The differences in observational error between tag-recapture and isotopic experiments have not been accounted for in the model. For some stock, such as PAU 5B (Breen 2003), the modelled stock status was sensitive to the growth estimates, depending on the choice of data or the modelling approach. The growth parameters, can be better determined if more and accurate growth data can be collected.

It was not known how well recruitment deviations were estimated. Breen (2003) suggested the actual recruitment fluctuations could be more extreme than those models suggested, as it takes a few years for paua to recruit into the fishery, and a strong impulse of year-class strengths could cover a wide length range.

5. ACKNOWLEDGMENTS

This work was supported by a contract from the Ministry of Fisheries (PAU2007-04 Objective 1). Thanks to Paul Breen for developing the stock assessment model that was used in this assessment and for the use of major proportions of the 2006 report for this update.

6. REFERENCES

Andrew, N.L.; Breen, P.A.; Naylor, J.R.; Kendrick, T.H.; Gerring, P. (2000). Stock assessment of paua (*Haliotis iris*) in PAU 7 in 1998–99. *New Zealand Fisheries Assessment Research Report 2000/49*. 40 p.

Breen, P.A.; Andrew, N.L.; Kendrick, T.H. (2000a). Stock assessment of paua (*Haliotis iris*) in PAU 5B and PAU 5D using a new length-based model. *New Zealand Fisheries Assessment Report 2000/33*. 37 p.

Breen, P.A.; Andrew, N.L.; Kendrick, T.H. (2000b). The 2000 stock assessment of paua (*Haliotis iris*) in PAU 5B using an improved Bayesian length-based model. *New Zealand Fisheries Assessment Report 2000/48*. 36 p.

Breen, P.A.; Andrew, N.L.; Kim, S.W. (2001). The 2001 stock assessment of paua (*Haliotis iris*) in PAU 7. *New Zealand Fisheries Assessment Report 2001/55*. 53 p.

Breen, P.A.; Kim, S.W. (2003). The 2003 stock assessment of paua (*Haliotis iris*) in PAU 7. *New Zealand Fishery Assessment Report 2003/35.* 112 p.

Breen, P.A.; Kim, S.W. (2004a). The 2004 stock assessment of paua (*Haliotis iris*) in PAU 4. *New Zealand Fisheries Assessment Report 2004/55.* 79 p.

Breen, P.A.; Kim, S.W. (2004b). The 2004 stock assessment of paua (*Haliotis iris*) in PAU 5A. *New Zealand Fisheries Assessment Report 2004/40*. 86 p.

Breen, P.A.; Kim, S.W. (2005). The 2005 stock assessment of paua (*Haliotis iris*) in PAU 7. *New Zealand Fisheries Assessment Report 2005/47.* 114 p.

Breen, P. A.; Kim, S.W. (2007). The 2006 stock assessment of paua (*Haliotis iris*) stocks PAU 5A (Fiordland) and PAU 5D (Otago). *New Zealand Fisheries Assessment Report 2007/09*. 164 p.

Breen, P.A.; Kim, S.W.; Andrew, N.L. (2003). A length-based Bayesian stock assessment model for abalone. *Marine and Freshwater Research 54(5):* 619–634.

Cordue, P.L. (2009). Analysis of PAU5A dive survey data and PCELR catch and effort data. Final report for SeaFIC and PauaMAC5. (Unpublished report held by the Ministry of Fisheries. SeaFIC.)

Dunn, A. (2007). Stock assessment of Foveaux Strait dredge oysters (*Ostrea chilensis*) for the 2005-06 fishing year. Final Research Report to the Ministry of Fisheries. Project OYS2007/01. 63 p. *(*Unpublished report held by the Ministry of Fisheries. Wellington.)

Fu, D.; A, McKenzie.; R, Naylor. (2010). Summary of input data for the 2010 PAU 5A stock assessment. *New Zealand Fisheries Assessment Report 2010/35*.

Gorfine, H.K.; Dixon, C.D. (2000) A behavioural rather than resource-focused approach may be need to ensure sustainability of quota managed abalone fisheries. *Journal of Shellfish Research* 19: 515–516.

Kim, S.W.; Bentley, N.; Starr, P.J.; Breen, P.A. (2004). Assessment of red rock lobsters (Jasus edwardsii) in CRA 4 and CRA 5 in 2003. *New Zealand Fisheries Assessment Report 2004/8.* 165 p.

McKenzie, A.; Smith, A.N.H. (2009). The 2008 stock assessment of paua (*Haliotis iris*) in PAU 7. New Zealand Fisheries Assessment Report 2009/34. 84 p.

Ministry of Fisheries Science Group (2009). Report from the Fisheries Assessment Plenary, May 2009: stock assessments and yield estimates. Ministry of Fisheries. Wellington, New Zealand. 990 p.

Punt, A.E. (2003). The performance of a size-structured stock assessment method in the face of spatial heterogeneity in growth. *Fisheries Research 65:* 391–409.

Schiel, D.R. (1989). Paua fishery assessment 1989. New Zealand Fisheries Assessment Research Document 89/9: 20 p. (Unpublished report held in NIWA library, Wellington, New Zealand.)

Schiel, D.R. (1992). The paua (abalone) fishery of New Zealand. *In* Abalone of the world: Biology, fisheries and culture. Shepherd, S.A.; Tegner, M.J.; Guzman del Proo,S. (eds.) pp. 427–437. Blackwell Scientific, Oxford.

Schiel, D.R.; Breen, P.A. (1991). Population structure, ageing and fishing mortality of the New Zealand abalone *Haliotis iris*. *Fishery Bulletin 89*: 681–691.

Shepherd, S.A.; Breen, P.A. (1992). Mortality in abalone: its estimation, variability and causes. In 'Abalone of the World: Biology, Fisheries and Culture'. (Eds S.A. Shepherd, M.J. Tegner, and S. Guzman del Proo.) pp. 276–304. (Blackwell Scientific: Oxford.)

Shepherd, S.A.; Partington, D. (1995). Studies on Southern Australian abalone (genus Haliotis). XVI. Recruitment, habitat and stock relations. *Marine and Freshwater Research 46*: 669–680.

Shepherd, S.A.; Rodda, K.R.; Vargas, K.M. (2001). A chronicle of collapse in two abalone stocks with proposals for precautionary management. Journal of Shellfish Research 20: 843–856.

Table 1: Actual sample sizes and effective sample sizes determined for the multinomial likelihood for the commercial catch proportions at length for Chalky and South Coast combined.

Year	Actual sample size	Effective sample size
1992	967	260
1993	831	330
1994	348	356
1998	157	157
2001	120	122
2002	1 823	832
2003	3 278	1 319
2004	2 010	762
2005	1 569	626
2006	1 126	384
2007	2 018	1 144
2008	431	297
2009	540	233

Table 2: Actual sample sizes and effective sample sizes determined for the multinomial likelihood for the research diver survey proportions at length for Chalky and South Coast combined.

Year	Actual sample size	Effective sample size
1996	811	328
2002	657	302
2003	637	155
2006	560	176
2008	93	44
2009	293	247

Table 3: Base case model specifications: for estimated parameters, the phase of estimation, lower bound, upper bound, type of prior, (U, uniform; N, normal; LN = lognormal), mean and c.v. of the prior.

Parameter	Phase	Prior	μ	c.v.	Bounds	
					Lower	Upper
			–	–		
ln(*R0*)	1	U	–	–	5	50
M	3	LN	0.1	0.1	0.01	0.5
g_{α}	2	U			1	50
g_{β}	2	U			0.01	50
ϕ	2	U			0.001	1
$\ln(q^{I})$	1	U			-30	0
X	1	U			0.05	10
$\ln(q^{J})$	1	U			-30	0
L_{50}	1	U			70	145
L_{95-50}	1	U			1	50
T_{50}	2	U			70	125
T_{95-50}	2	U			0.001	50
D_{50}	2	U			70	145
D_{95-50}	2	U			0.01	50
ε	1	N	0	0.4	0.01	1

Table 4: Values for fixed quantities for base case model.

Variable	Value
α	75
β	120
a	2.99E-08
b	3
$U^{\max}$	0.65
σ_{MIN}	1.0
σ_{obs}	0.25
h	1
$\tilde{\sigma}$	0.2
ϖ^{I}	0.16
ϖ^{I2}	0.21
ϖ^{J}	0.23
ϖ^{r}	0.14
ϖ^{s}	0.21
ϖ^{tag}	0.14
ϖ^{mat}	3.85

Table 5: Summary descriptions for base case and sensitivity model runs.

Mode runs	Descriptions
1.0 (Base case)	Base case catch history estimates, CSLF 2002–2005, and ε estimated for 1986–2006
1.1	Base case, but up-weighted the CPUE dataset
1.2	Base case, but estimated recruitment deviation for 1992-2006
2.0	Base case, but with CSLF 1991–94, 98, and 2001–09, and ε for 1982-2006
3.0	Base case, but excluded all CSLF
4.0	Base case, but with upper bound catch history estimates
5.0	Base case, but with lower bound catch history estimates
5.1	Base case, but with lower bound catch history estimates, and up-weighted CPUE dataset

Table 6: MPD estimates for base case and sensitivity trials. SDNRs: standard deviations of the normalised residuals. Shading indicates SDNRs inflated because they were not estimated, likelihood contributions not used when datasets were removed, and parameter fixed at the base case estimates.

Model runs	1.0	1.1	1.2	2.0	3.0	4.0	5.0	5.1
Weights								
CPUE	0.16	0.4	0.12	0.04	0.23	0.32	0.07	0.4
PCPUE	0.21	0.22	0.22	0.11	0.18	0.22	0.2	0.2
RDSI	0.23	0.23	0.23	0.24	0.23	0.23	0.22	0.22
CSLF	0.21	0.21	0.21	0.14	0.04	0.22	0.2	0.2
RDLF	0.34	0.35	0.34	0.32	0.38	0.34	0.33	0.33
Tags	3.85	3.85	3.85	3.85	3.85	3.85	3.85	3.85
Maturity	0.14	0.14	0.14	0.14	0.13	0.14	0.12	0.12
SDNRs								
sdnrCPUE	1.02	1.40	1.01	0.95	1.00	1.00	1.00	1.84
sdnrPCPUE	0.99	1.04	0.98	0.65	1.01	1.01	1.02	1.01
sdnrRDSI	1.00	1.00	1.00	1.03	1.00	1.00	0.99	0.97
sdnrCSLF	1.00	1.01	1.00	0.95	0.79	1.00	0.97	1.07
sdnrRDLF	1.00	1.03	1.01	0.97	1.01	1.01	1.00	1.04
sdnrMaturity	1.00	1.00	1.00	1.00	1.00	1.00	1.00	1.00
sdnrTags	1.02	1.00	1.02	1.03	1.05	1.02	1.04	1.05
Likelihoods								
CPUE	-11.6	-17.1	-8.2	4.3	-16.2	-20.1	-1.9	-8.4
PCPUE	-9.7	-9.7	-10.2	-6.8	-8.3	-9.9	-9.1	-9.2
RDSI	1.4	1.3	1.3	1.3	1.3	1.3	1.5	1.4
CSLF	54.1	55.6	54.4	153.8	32.7	54.1	52.2	61.5
RDLF	119.1	125.8	120.6	109.0	117.2	119.2	116.8	129.0
Tags	853.5	857.2	852.2	852.4	848.4	853.8	845.8	853.2
Maturity	-16.7	-16.7	-16.7	-16.7	-16.7	-16.7	-16.7	-16.7
Prior on M	0.4	0.3	1.0	3.8	0.5	-1.1	7.0	14.2
Prior on ε	6.7	8.1	6.7	19.1	7.8	4.2	11.8	12.9
U penalty	0.0	0.0	0.0	0.0	0.0	0.0	0.0	0.0
Total likelihood	997.1	1004.9	1001.2	1120.3	934.1	984.8	1007.5	1038.1
Parameters	1.0	1.1	1.2	2.0	3.0	4.0	5.0	5.1
ln($R0$)	12.71	12.70	12.73	12.66	12.72	12.77	12.79	13.12
M	0.12	0.12	0.12	0.14	0.12	0.11	0.15	0.17
T_{50}	107.91	108.91	107.30	107.14	107.30	107.96	106.78	110.31
$T_{95\text{-}50}$	18.15	18.23	17.82	18.03	20.02	18.19	17.52	18.24
D_{50}	126.26	126.40	126.16	125.61	126.26	126.16	126.19	126.67
$D_{95\text{-}50}$	5.59	5.73	5.50	4.98	5.59	5.47	5.53	6.00
L_{50}	91.79	91.79	91.79	91.79	91.79	91.79	91.79	91.79
$L_{95\text{-}50}$	19.58	19.58	19.58	19.58	19.58	19.58	19.58	19.58
ln(q^I)	-12.55	-12.46	-12.63	-12.44	-12.43	-12.55	-12.79	-12.65
X	1.29	1.32	1.29	0.98	1.07	1.30	1.28	1.34
ln(q^J)	-12.55	-12.46	-12.63	-12.44	-12.43	-12.55	-12.79	-12.65
g_α	23.05	22.25	23.71	23.65	25.14	22.75	25.11	23.32
g_β	7.37	7.64	7.23	7.27	7.11	7.38	7.01	7.67
φ	0.29	0.29	0.29	0.29	0.26	0.29	0.24	0.23

Table 6–continued

Indicators								
B_0	1142	1102	1247	1090	1150	1336	1002	848
B_{init}	1014	1029	985	784	1009	1280	773	872
$B_{\min}$	371	341	402	343	378	366	451	431
$B_{current}$	384	357	413	382	407	394	451	444
$B_{current}/B_0$	0.34	0.32	0.33	0.35	0.35	0.30	0.45	0.52
$B_{current}/B_{init}$	0.38	0.35	0.42	0.49	0.40	0.31	0.58	0.51
$B_{current}/B_{\min}$	1.04	1.05	1.03	1.11	1.08	1.08	1.00	1.03
B_0^r	998	969	1082	927	1001	1189	829	686
B_{init}^r	886	905	855	666	879	1139	639	705
$B_{\min}^r$	196	175	221	187	200	220	295	244
$B_{current}^r$	228	208	250	237	243	267	319	290
$B_{current}^r/B_0^r$	0.23	0.22	0.23	0.26	0.24	0.22	0.38	0.42
$B_{current}^r/B_{init}^r$	0.26	0.23	0.29	0.36	0.28	0.23	0.50	0.41
$B_{current}^r/B_{\min}^r$	1.17	1.19	1.13	1.27	1.21	1.21	1.08	1.19
min*Rdev*	0.65	0.50	0.77	0.71	0.59	0.66	0.69	0.33
max*Rdev*	1.67	1.72	1.83	2.73	1.74	1.47	1.93	1.57
$U_{current}$	0.22	0.24	0.20	0.21	0.21	0.22	0.19	0.21

Table 7: Correlations among estimated parameters for the base case MCMC. Boxes indicate absolute values greater than 0.50.

Parameter	$\ln(R0)$	M	g_α	g_β	T_{50}	$T_{95\text{-}50}$	D_{50}	$D_{95\text{-}50}$	L_{50}	$L_{95\text{-}50}$	φ	$\ln(q^I)$	X	$\ln(q^J)$
$\ln(R0)$	1.00													
M	0.94	1.00												
g_α	-0.06	-0.05	1.00											
g_β	-0.21	0.05	0.09	1.00										
T_{50}	0.30	0.34	-0.39	0.11	1.00									
$T_{95\text{-}50}$	0.06	0.05	-0.07	-0.10	0.32	1.00								
D_{50}	0.07	0.06	-0.19	-0.08	0.16	0.07	1.00							
$D_{95\text{-}50}$	0.01	0.01	-0.07	-0.05	0.07	0.04	0.67	1.00						
L_{50}	0.00	0.00	0.00	0.00	0.00	0.00	0.00	0.00	1.00					
$L_{95\text{-}50}$	0.00	0.00	0.00	0.00	0.00	0.00	0.00	0.00	-0.33	1.00				
φ	0.08	-0.01	-0.24	-0.41	0.03	0.07	0.06	0.01	0.00	0.00	1.00			
$\ln(q^I)$	-0.55	-0.36	-0.29	0.61	0.16	0.01	0.14	0.10	0.00	0.00	-0.14	1.00		
X	-0.08	-0.12	0.07	-0.08	0.00	0.06	0.17	0.10	0.00	0.00	0.03	-0.19	1.00	
$\ln(q^J)$	-0.33	-0.24	-0.11	0.30	0.18	0.08	0.02	0.01	0.00	0.00	-0.07	0.41	0.18	1.00

Table 8 : Summary of the marginal posterior distributions from the MCMC chain from the base case. The columns show the minimum values observed in the 1000 samples, the maxima, the 5th and 95th percentiles, and the medians. Biomass is in tonnes.

	Min	5%	Median	95%	Max
SDNRs					
sdnrCPUE	0.65	0.82	1.11	1.39	1.73
sdnrCPUE2	0.74	0.88	1.04	1.23	1.40
sdnrRDSI	0.92	0.97	1.01	1.07	1.13
sdnrCSLF	0.96	0.99	1.03	1.09	1.13
sdnrRDLF	0.98	1.00	1.03	1.05	1.09
sdnrmat	1.00	1.00	1.04	1.16	1.34
sdnrtags	0.86	0.92	0.99	1.06	1.12
Parameters					
f	1004.74	1008.86	1015.20	1022.56	1038.11
ln(*R0*)	12.37	12.53	12.74	12.96	13.16
M	0.10	0.11	0.12	0.14	0.15
T_{50}	102.93	105.43	107.70	109.93	113.09
$T_{95\text{-}50}$	11.07	15.07	18.55	23.28	28.33
D_{50}	125.42	125.81	126.25	126.76	127.29
$D_{95\text{-}50}$	4.08	4.90	5.64	6.45	7.31
L_{50}	87.75	89.98	91.65	93.33	94.95
$L_{95\text{-}50}$	13.02	16.31	19.91	24.38	29.04
$\ln(q^I)$	-12.85	-12.75	-12.59	-12.46	-12.30
X	1.05	1.16	1.29	1.44	1.60
$\ln(q^J)$	-14.49	-14.26	-14.02	-13.77	-13.57
g_α	19.85	21.24	23.27	25.40	28.35
g_β	6.66	6.91	7.25	7.60	8.01
φ	0.25	0.28	0.30	0.33	0.36
Indicators					
B_0	996	1066	1155	1252	1345
B_{init}	906	962	1025	1088	1152
$B_{\min}$	285	331	382	447	513
$B_{current}$	288	338	397	478	567
$B_{current}/B_0$	0.24	0.28	0.35	0.42	0.49
$B_{current}/B_{init}$	0.30	0.34	0.39	0.45	0.54
$B_{current}/B_{\min}$	1.00	1.01	1.04	1.10	1.24
B_0^r	844	913	1007	1111	1206
B_{init}^r	776	835	894	945	999
$B_{\min}^r$	140	172	204	251	300
$B_{current}^r$	170	201	237	286	349
$B_{current}^r/B_0^r$	0.16	0.19	0.24	0.29	0.36
$B_{current}^r/B_{init}^r$	0.20	0.22	0.27	0.32	0.39
$B_{current}^r/B_{\min}^r$	1.02	1.08	1.16	1.25	1.34
$U_{current}$	0.15	0.18	0.22	0.25	0.29

Table 9: Summary of key indicators from the projection for the base case MCMC: projected biomass as a percentage of the virgin and current stock status, for spawning stock and recruit-sized biomass, respectively.

Projection	2009	2010	2011	2012
$\% B_0$	34.6 (27.3-43.9)	35.6 (27.8-45.2)	37.5 (29.3-47.7)	39.4 (30.9-50)
$\% B_0^r$	20.7 (16.3-25.8)	21.5 (16.7-27.1)	22.2 (17.1-28.4)	23.2 (17.9-30)
$\% B_{current}$	100 (100-100)	103 (99-107)	108 (100-117)	114 (102-126)
$\% B_{current}^r$	100 (100-100)	104 (99-110)	108 (100-117)	112 (103-123)

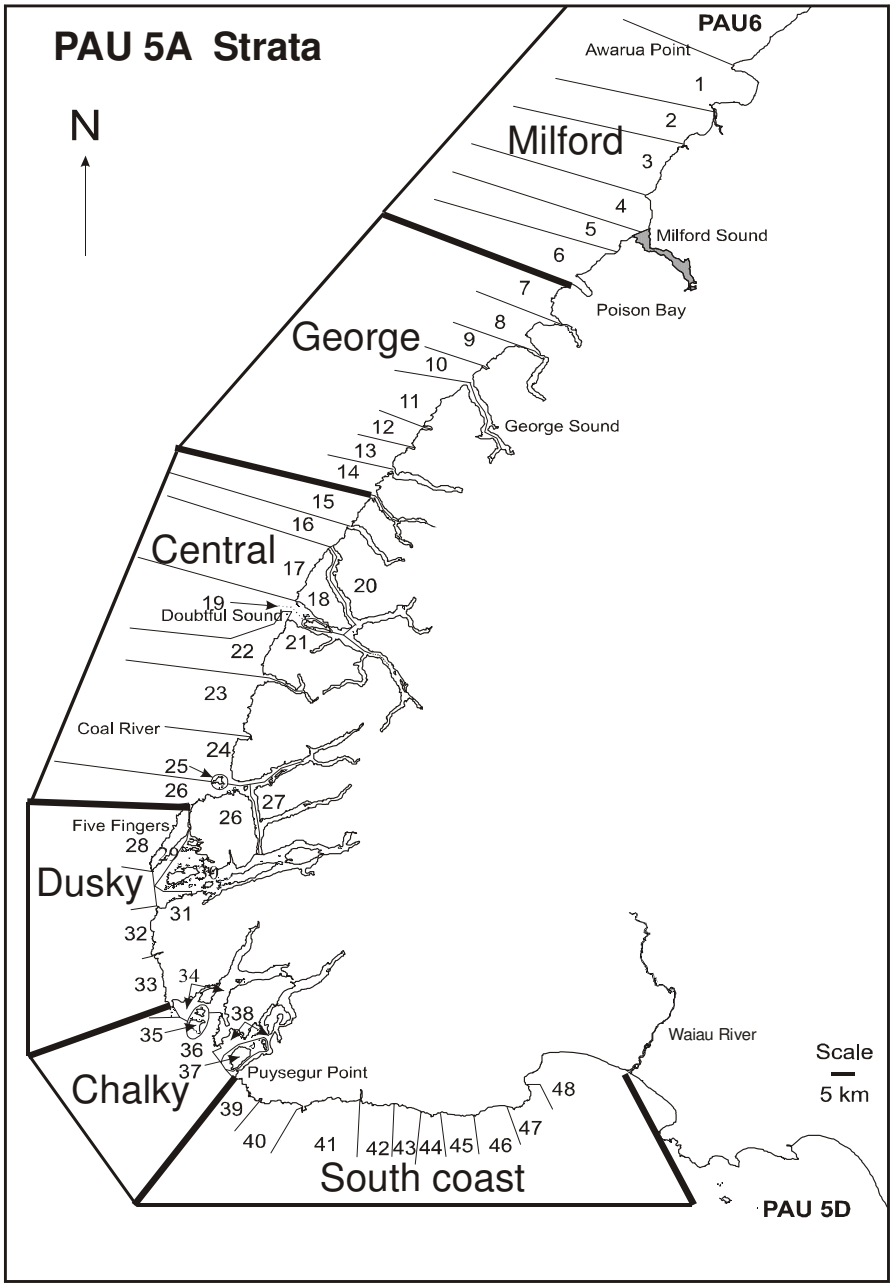

Figure 1: Boundaries of PAU 5A, fine-scale statistical area and research survey strata.

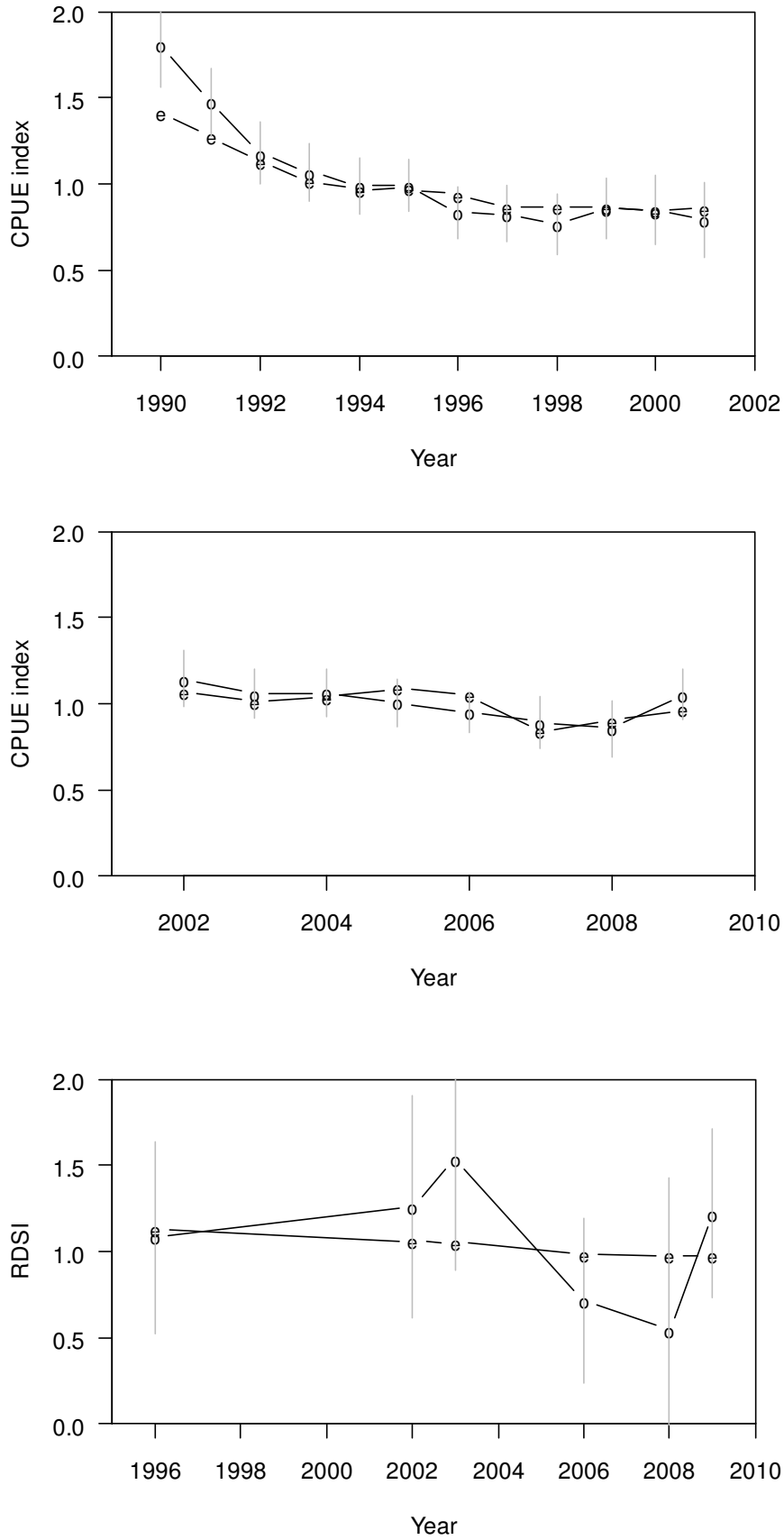

Figure 2: Observed (dots) and predicted (solid line) CPUE (top), PCPUE (middle), and RDSI (bottom) for the base case MPD fit. Error bars show the standard error term used by the model in fitting, including the effects of the common error term and the dataset weights.

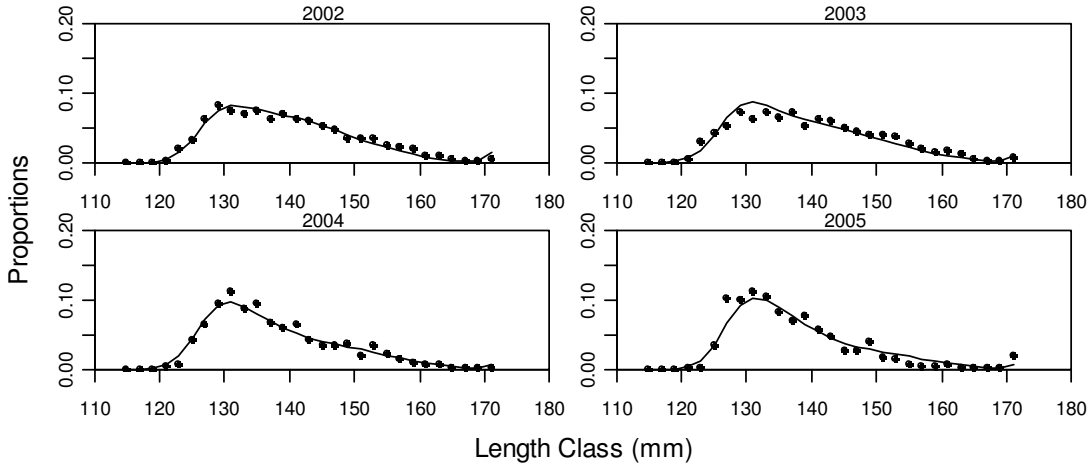

Figure 3: Observed (dots) and predicted (lines) proportions-at-length from commercial catch sampling (CSLF) from the base case MPD fits.

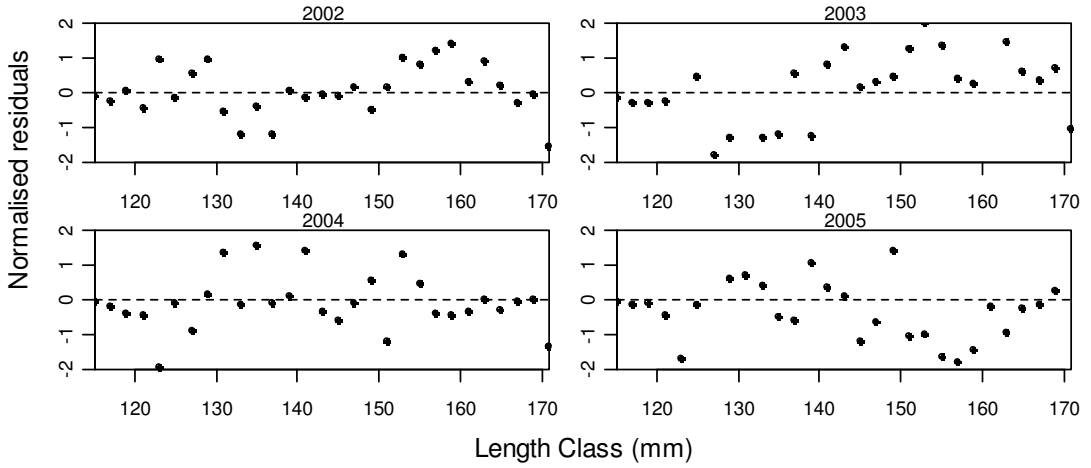

Figure 4: Residuals from base case MPD fits to CSLF data seen in Figure 3.

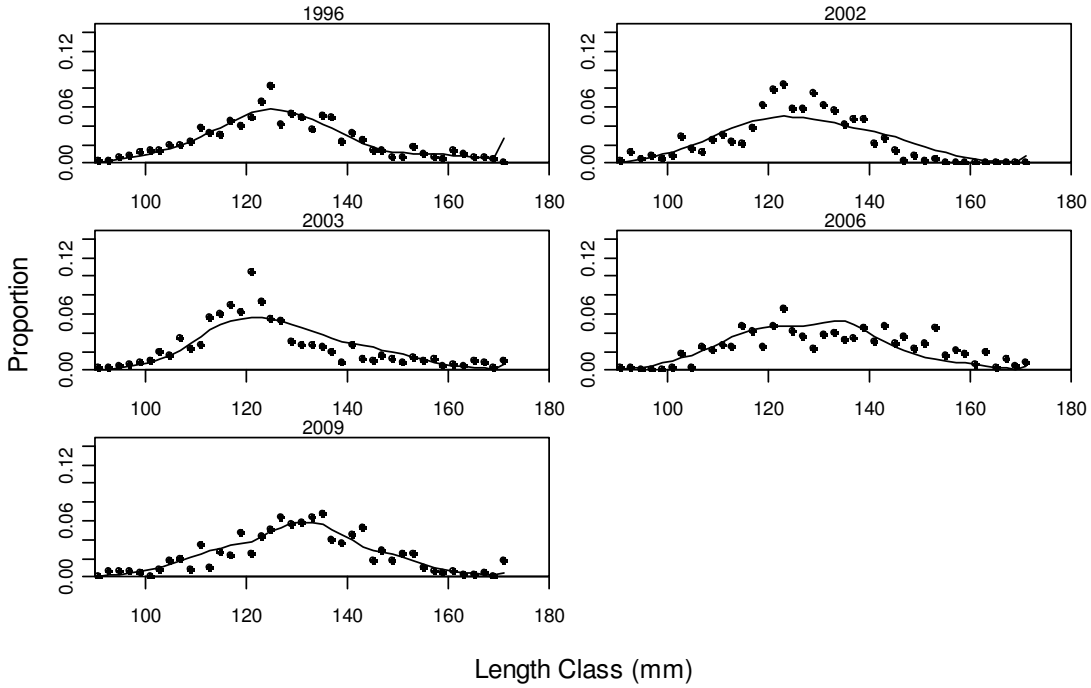

Figure 5: Observed (dots) and predicted (lines) proportions-at-length from research diver survey catch sampling (RDLF) from the base case MPD fits.

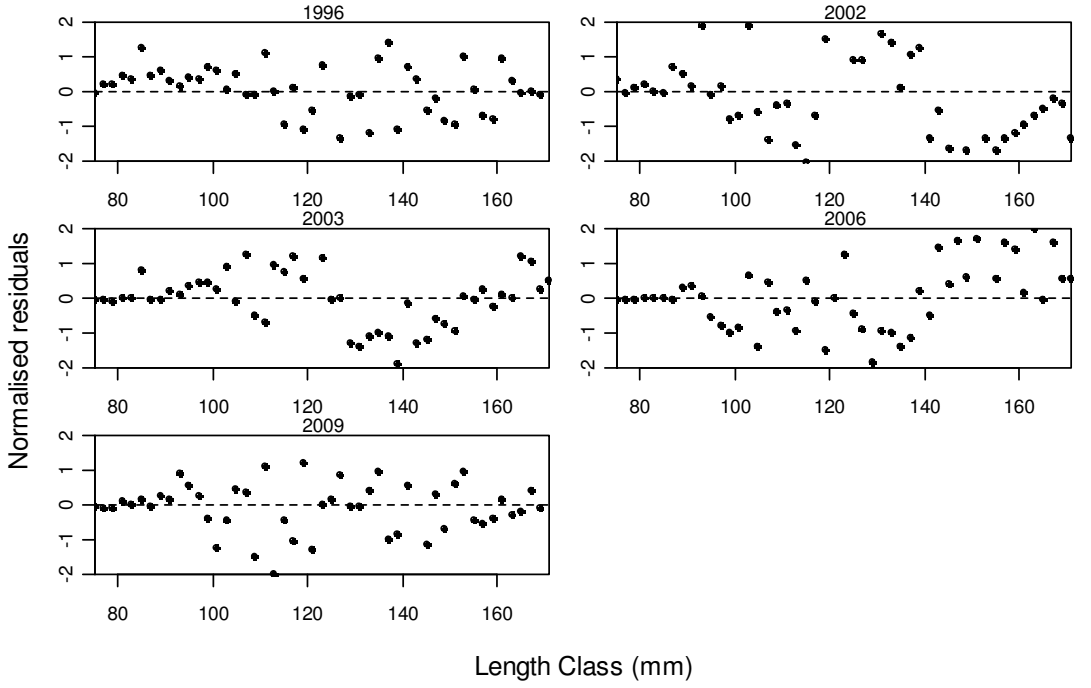

Figure 6: Residuals from base case MPD fits to RDLF data seen in Figure 5.

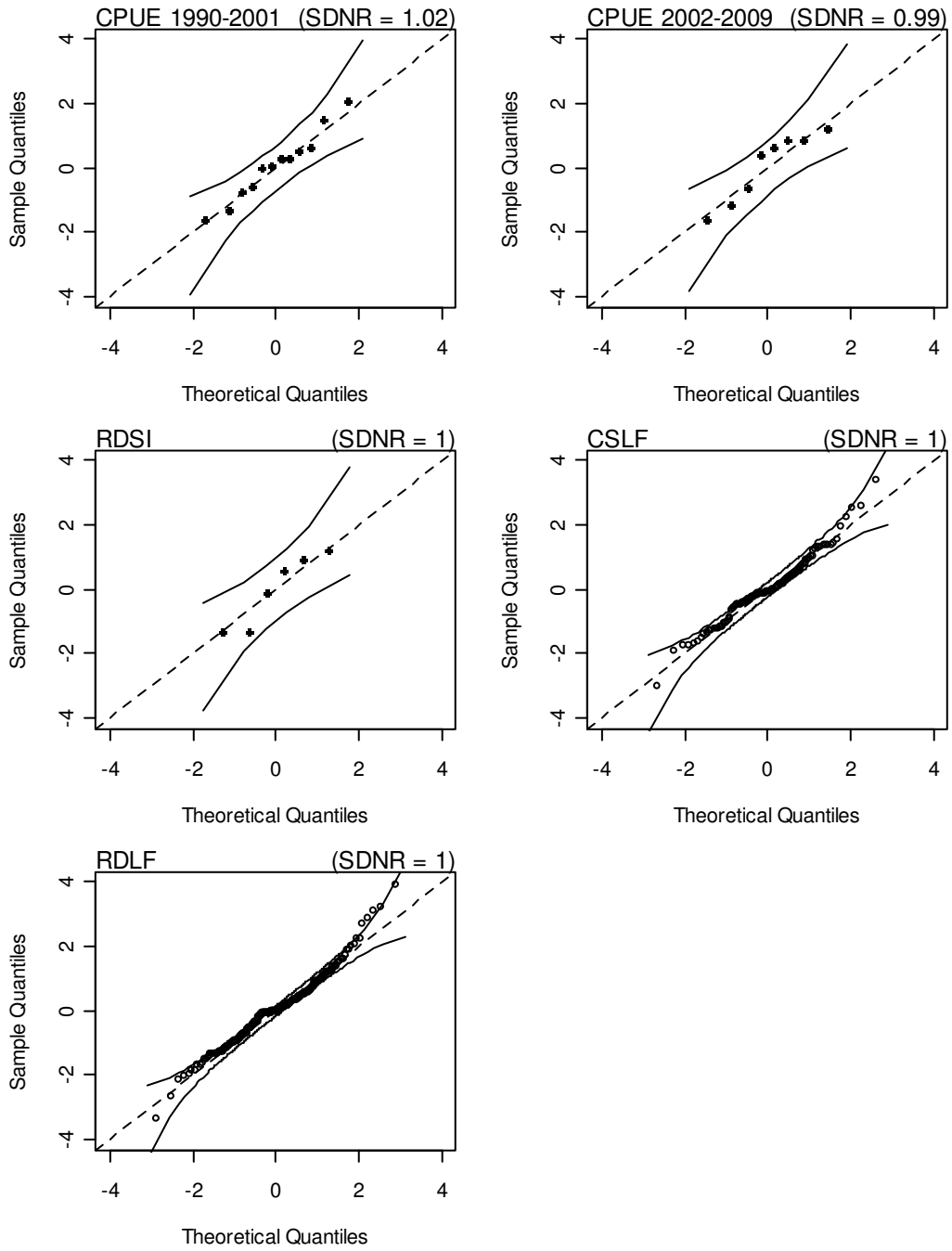

Figure 7: Q-Q plot of residuals for the fits to the CPUE, PCPUE, RDSI, CSLF, and RDLF from the base case MPD fit.

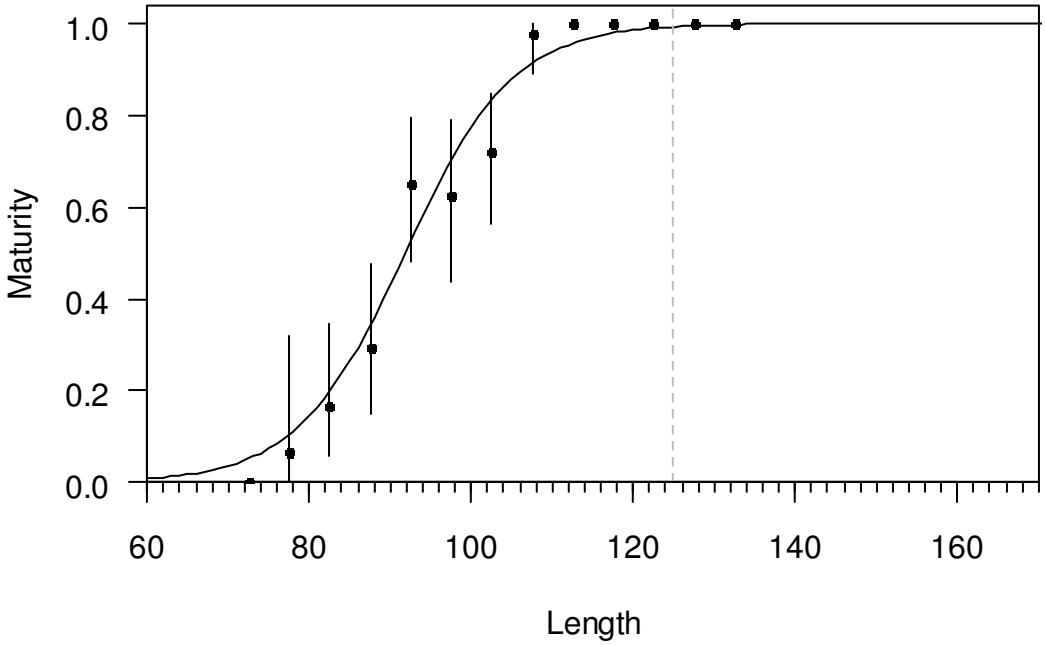

Figure 8: Observed (dots and vertical bars) and predicted proportion of maturity at length for the base case MPD fit. Vertical bars represent 95% interval of estimated proportion mature at each length bin. Dashed line represents the legal size limit of 125 mm.

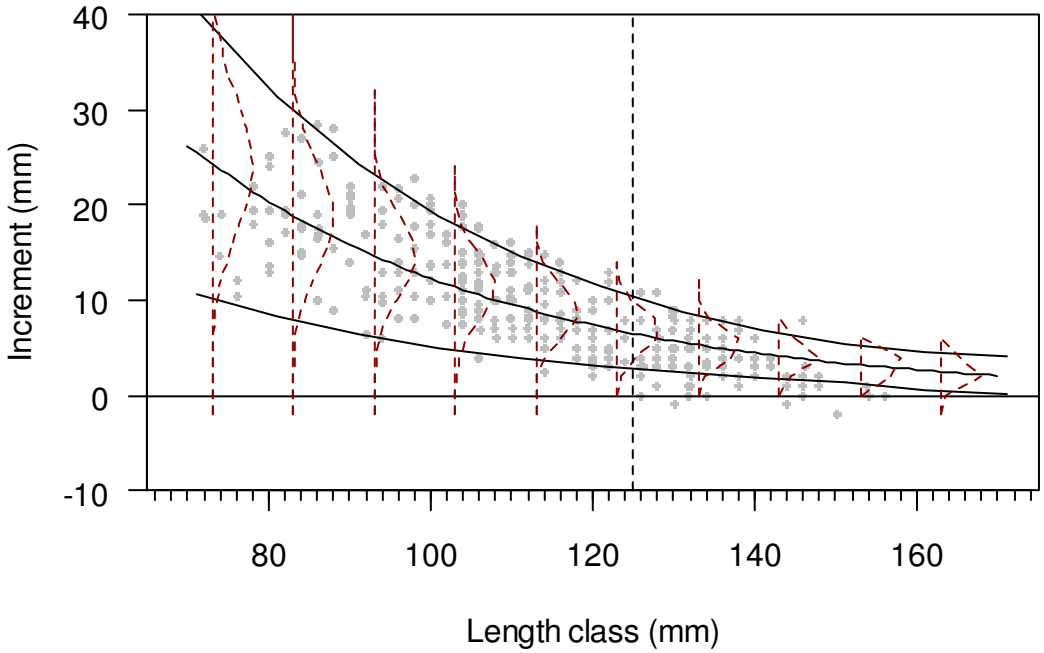

Figure 9: Observed mean annual increment at size from the growth data (dots), model estimated growth curve with 95% confidence interval (black lines), and model estimated growth transition matrix at selected sizes (dashed lines) for the base case MPD fit. The dashed vertical line represents the legal size limit of 125 mm.

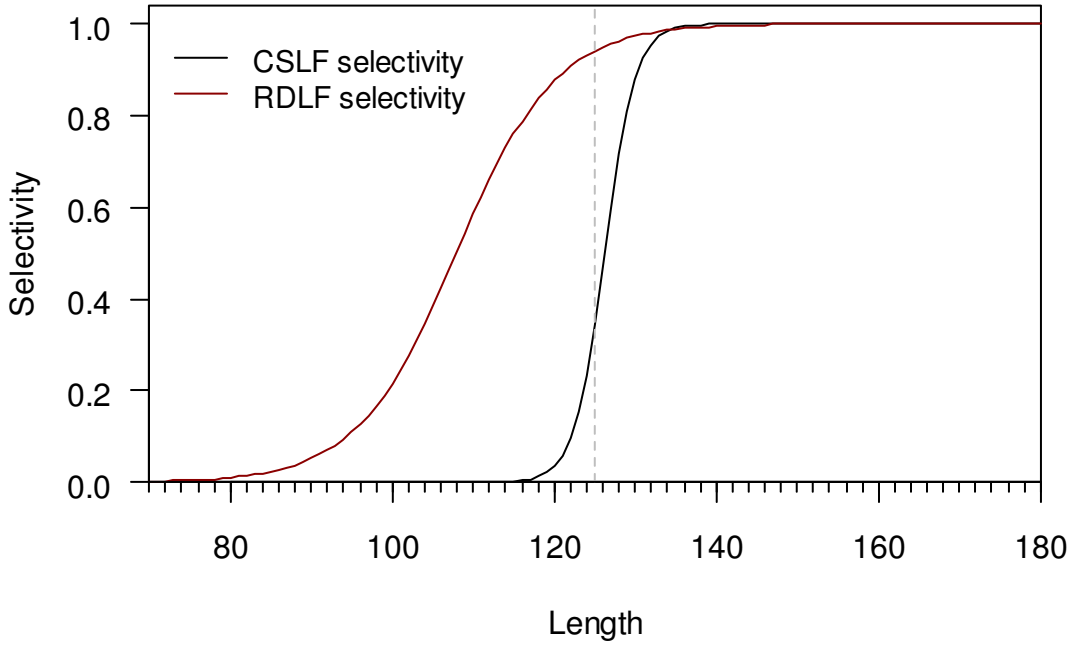

Figure 10: Estimated commercial and research diver selectivity from base case MPD fits. Dashed line represents the legal size limit of 125 mm.

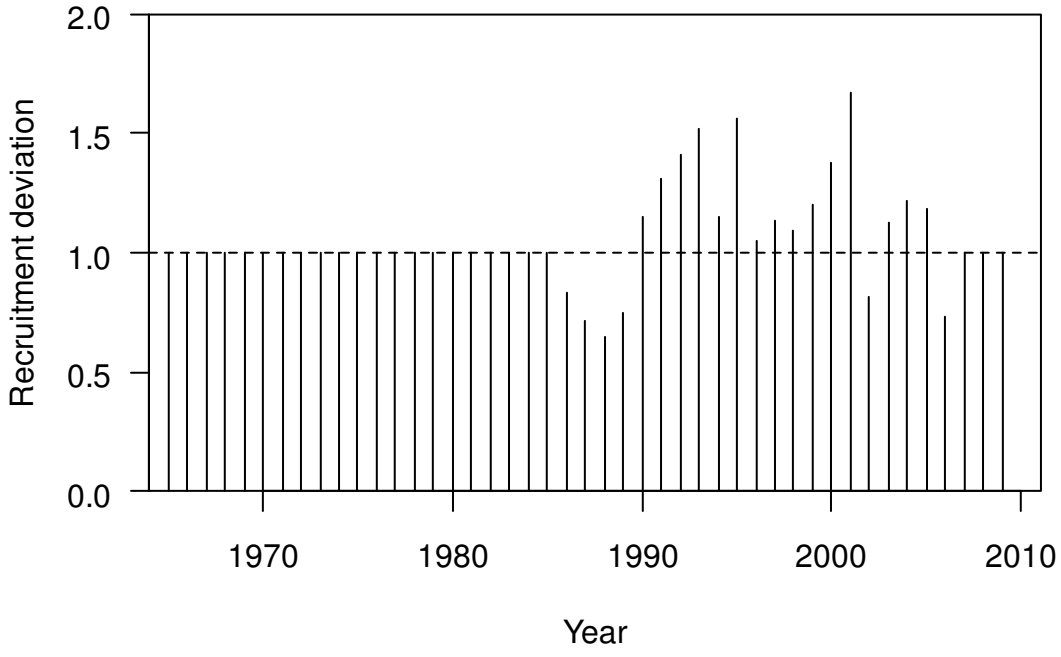

Figure 11: Recruitment deviations from base case MPD fits. Recruitment deviations were estimated for 1986–2006, and assumed to be fixed at 1 for other years.

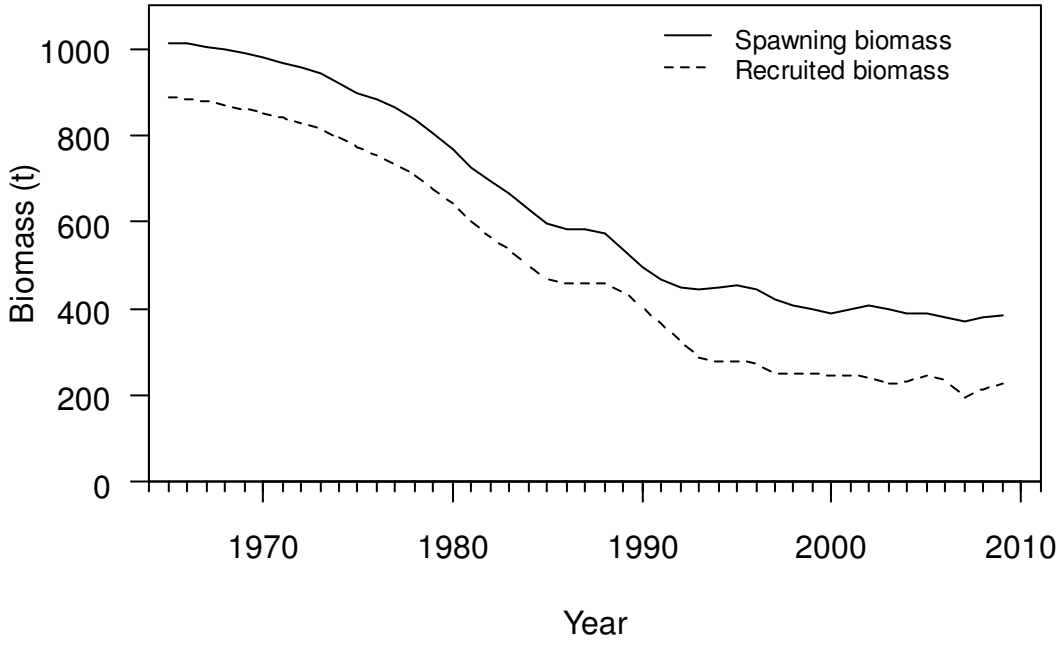

Figure 12: Spawning and recruited biomass trajectory from the base case MPD fit.

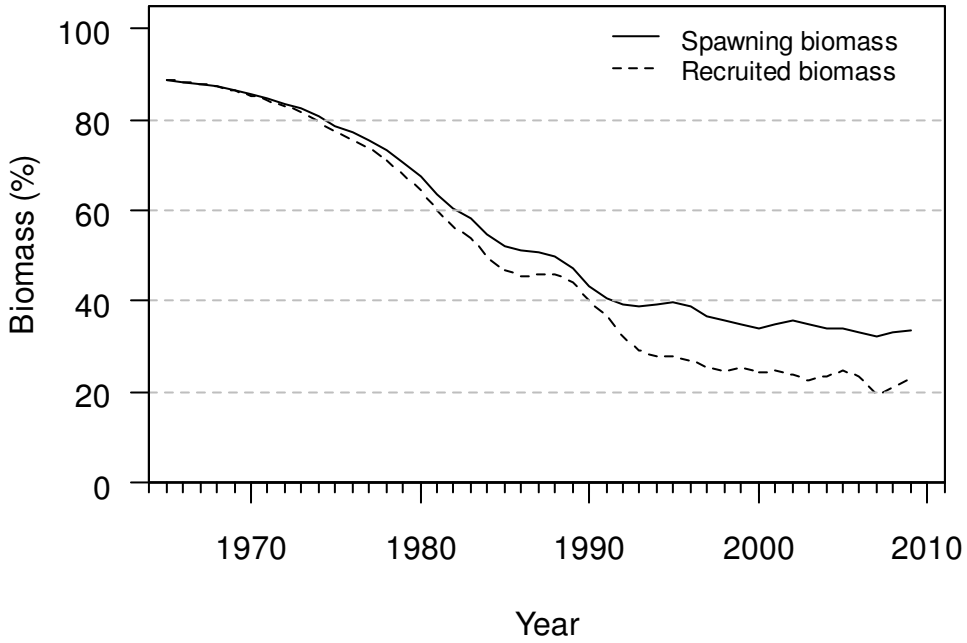

Figure 13: Spawning stock biomass as a percentage of B_0 and recruited biomass as a percentage of B_0^r from the base case MPD fit.

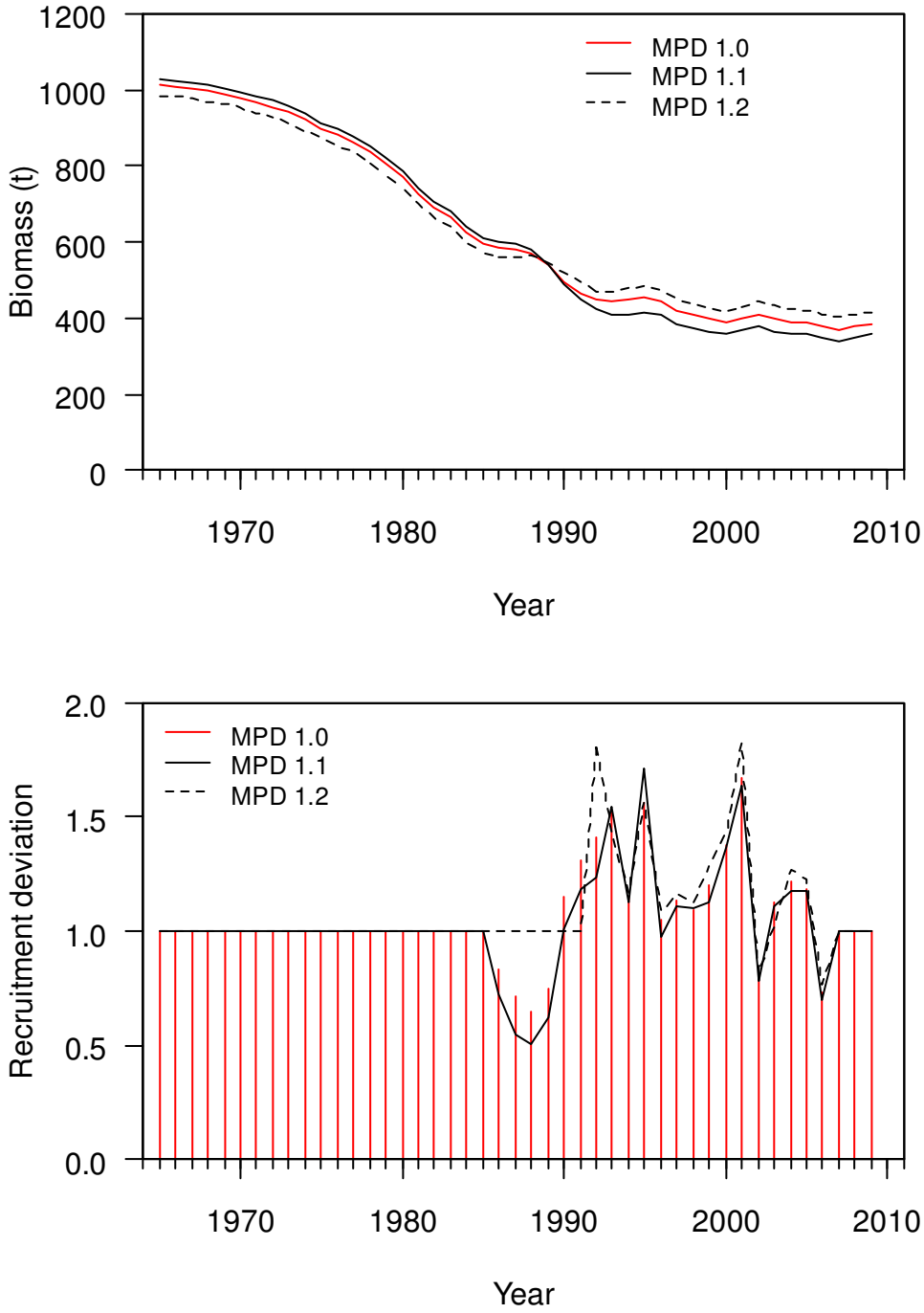

Figure 14: A comparison of MPD estimates of spawning stock biomass (top) and recruitment deviations (bottom) for base case model(1.0) and sensitivity trials 1.1, and 1.2.

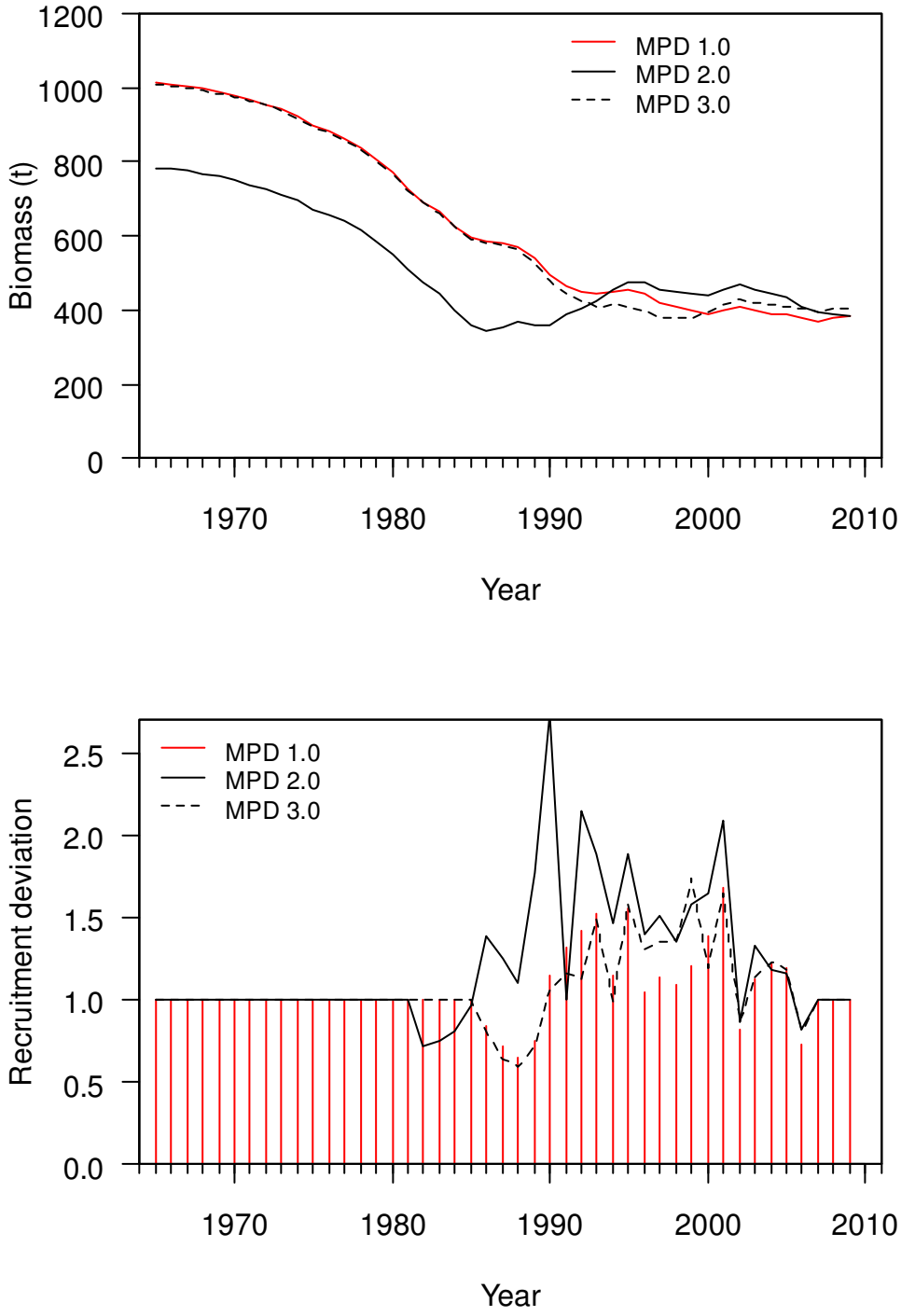

Figure 15: A comparison of MPD estimates of spawning stock biomass (top) and recruitment deviations (bottom) for base case model(1.0) and sensitivity trials 2.0, and 3.0.

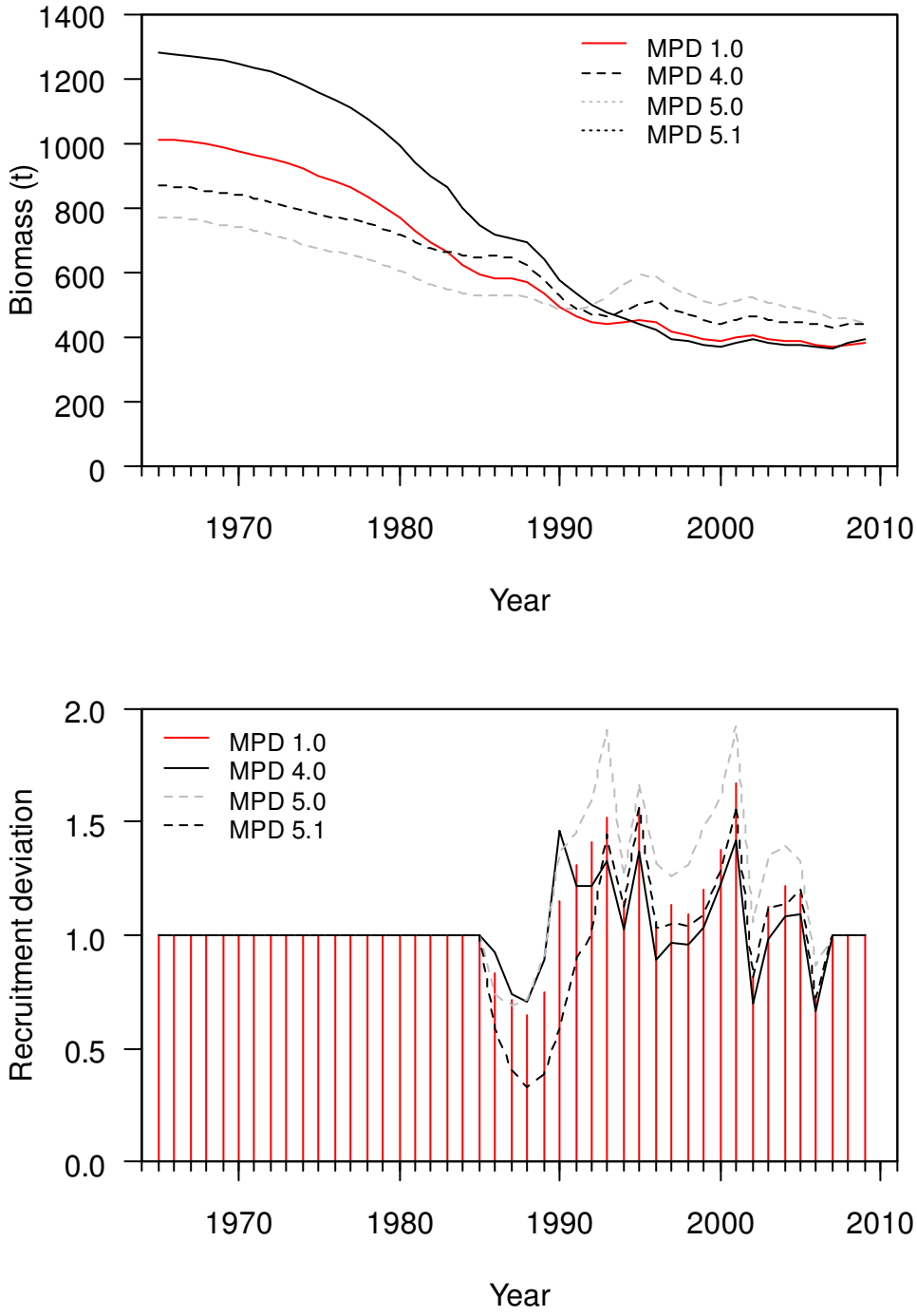

Figure 16 : A comparison of MPD estimates of spawning stock biomass (top) and recruitment deviations (bottom) for base case model(1.0) and sensitivity trials 4.0, and 5.0, and 5.1.

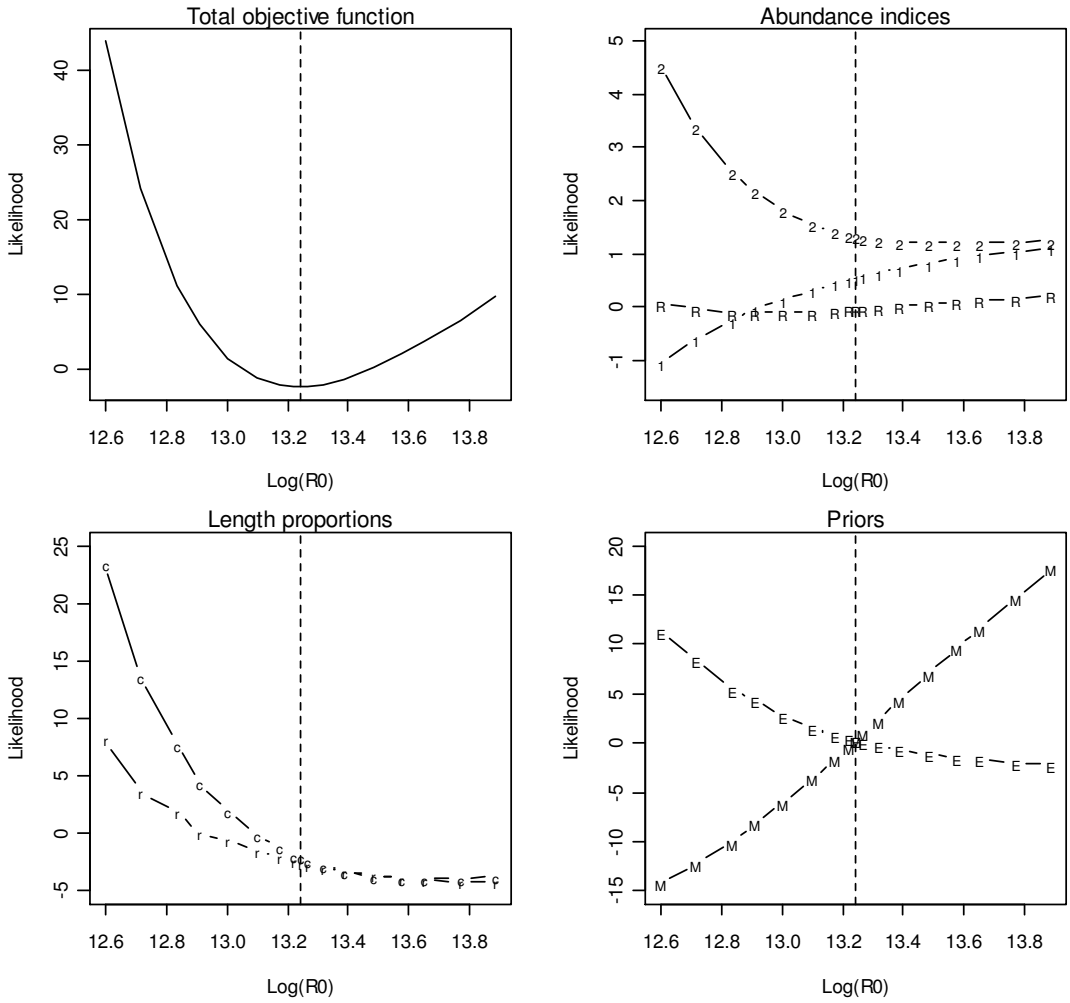

Figure 17: Likelihood profile of parameter Ln(R_0) based on a variation of sensitivity run 2.0. A penalty function was added to encourage the average recruitment deviations to be close to 1. The left upper panel shows the total objective function value and, and the rest show the objective function value for individual components. 1, CPUE data; 2, PCPUE data; R, RDSI data; r, RDLF data; c, CSLF data; E, prior on recruitment deviations; M, prior on natural mortality.

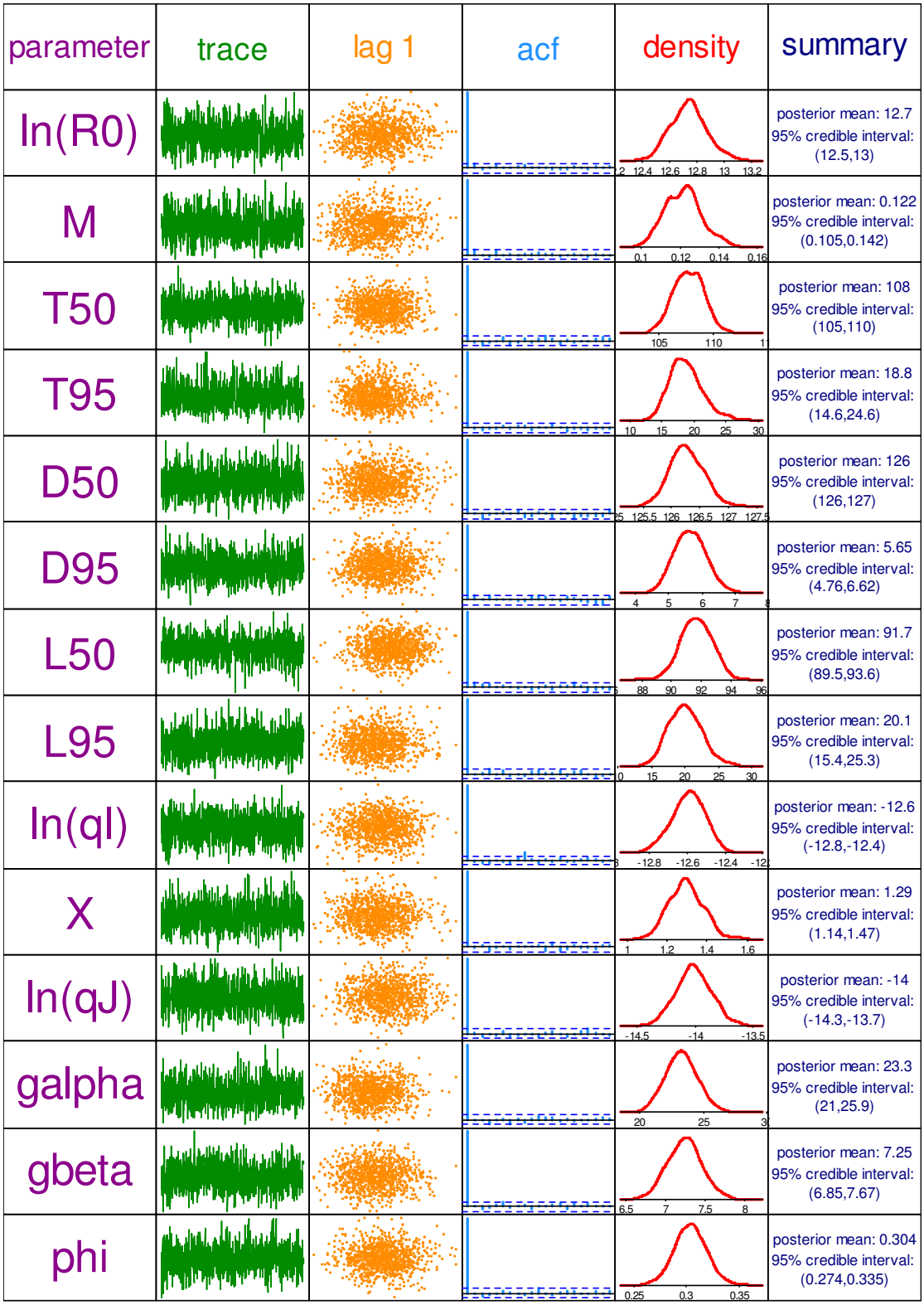

Figure 18: Diagnostics for the base case MCMC posterior samples of estimated parameters and indicators. "trace" is the trace plot of the sampled chain; "lag 1" is the i^{th} data plotted against the $i+1^{th}$ data in the chain; "acf" is the autocorrelation of the chain at lag 1, 2, …; "density" is the posterior distribution.

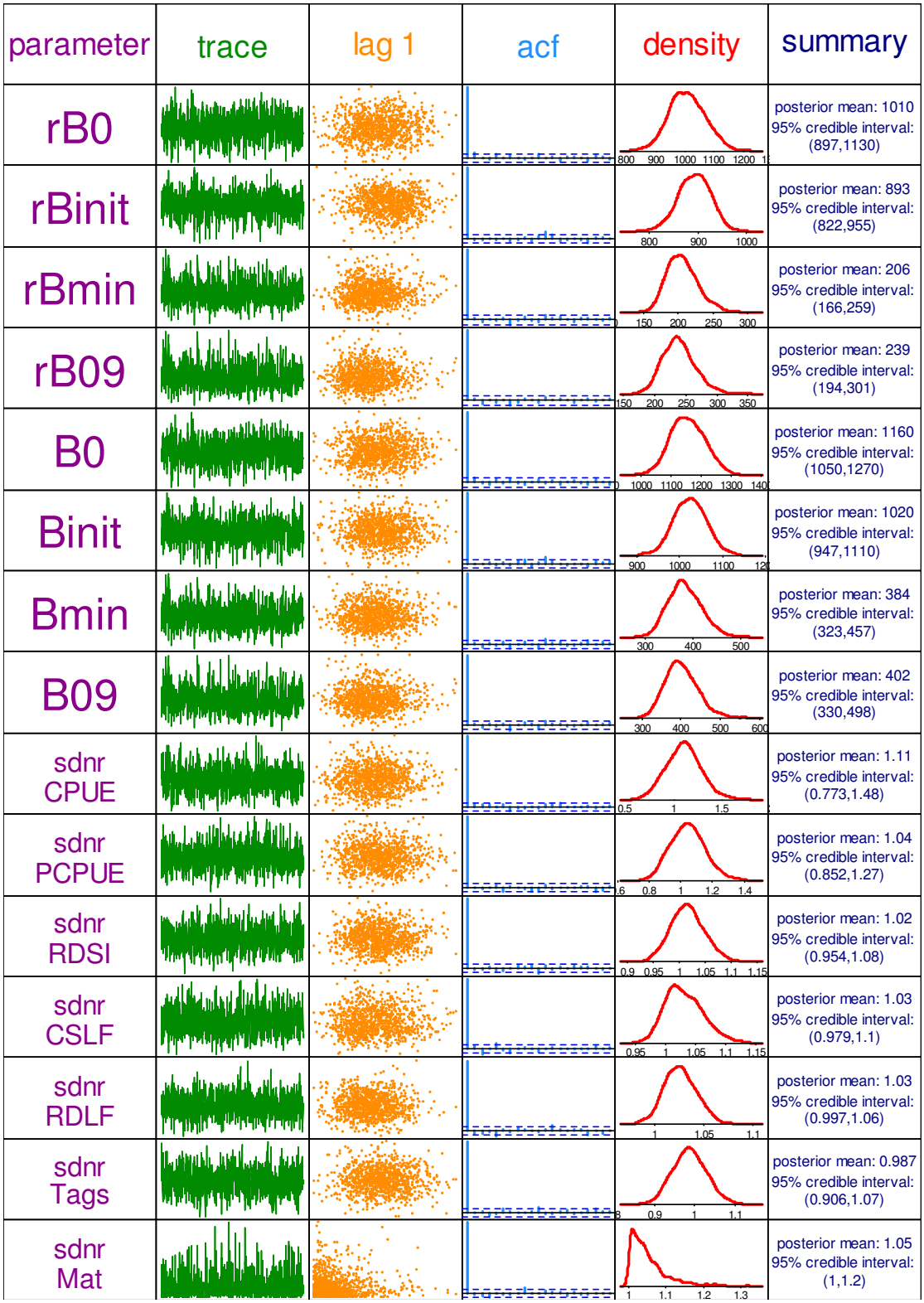

Figure 18–continued.

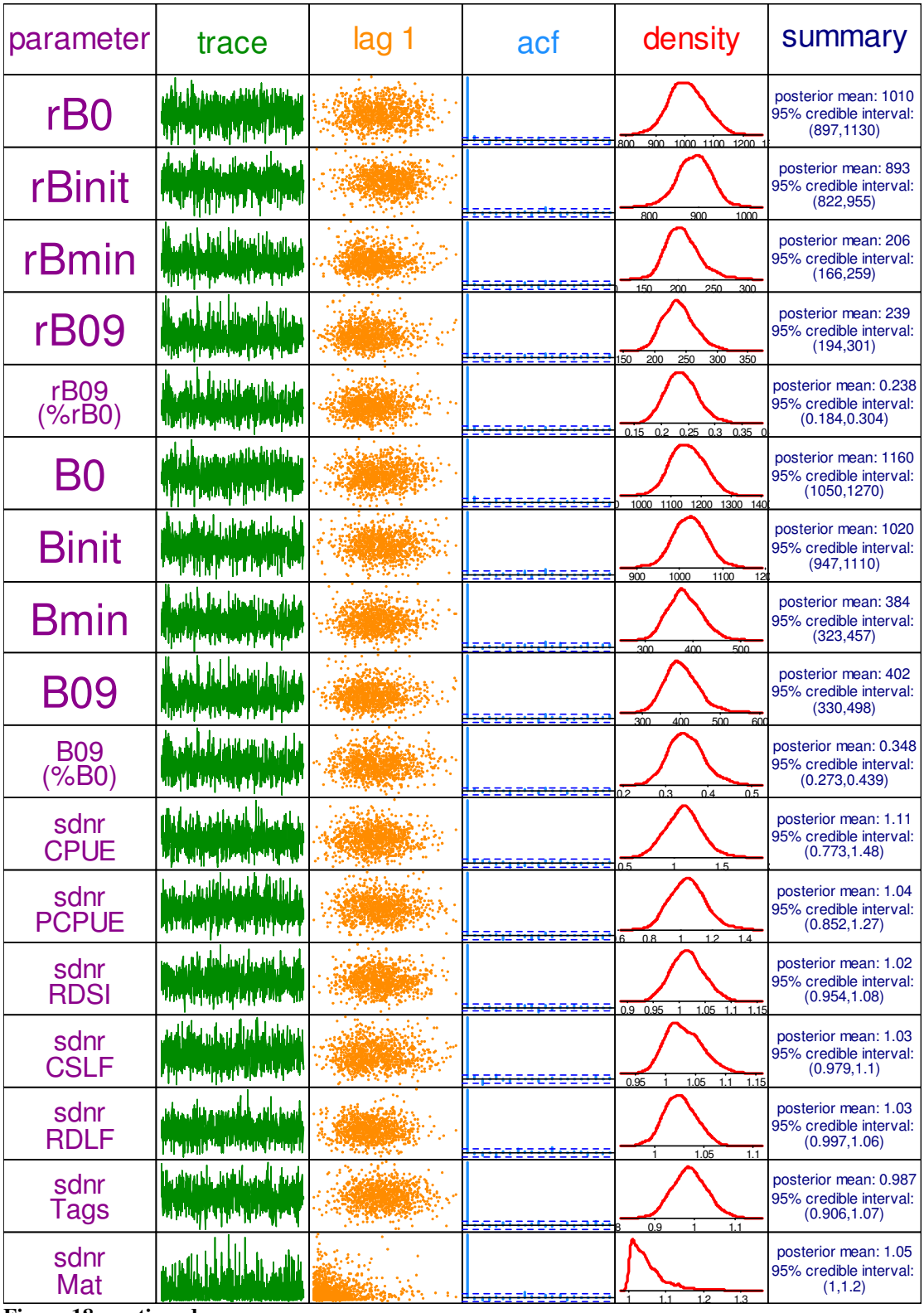

Figure 18–continued.

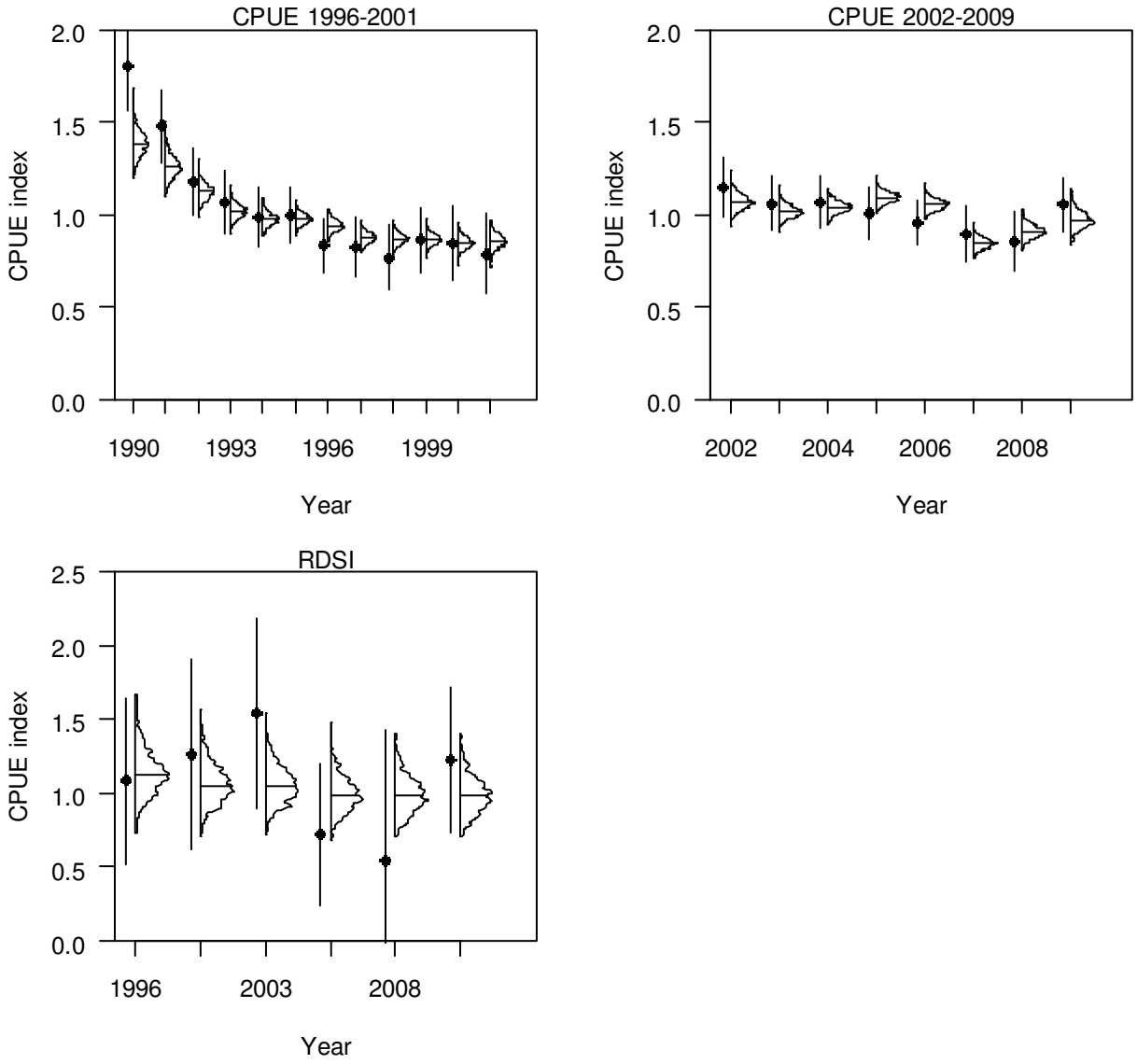

Figure 19: The posterior distributions of the fits to the CPUE, PCPUE, and RDSI data for the base case MCMC. The dots are the observed data. Error bars show the standard error term used by the MPD model in fitting, including the effects of the common error term and the dataset weights.

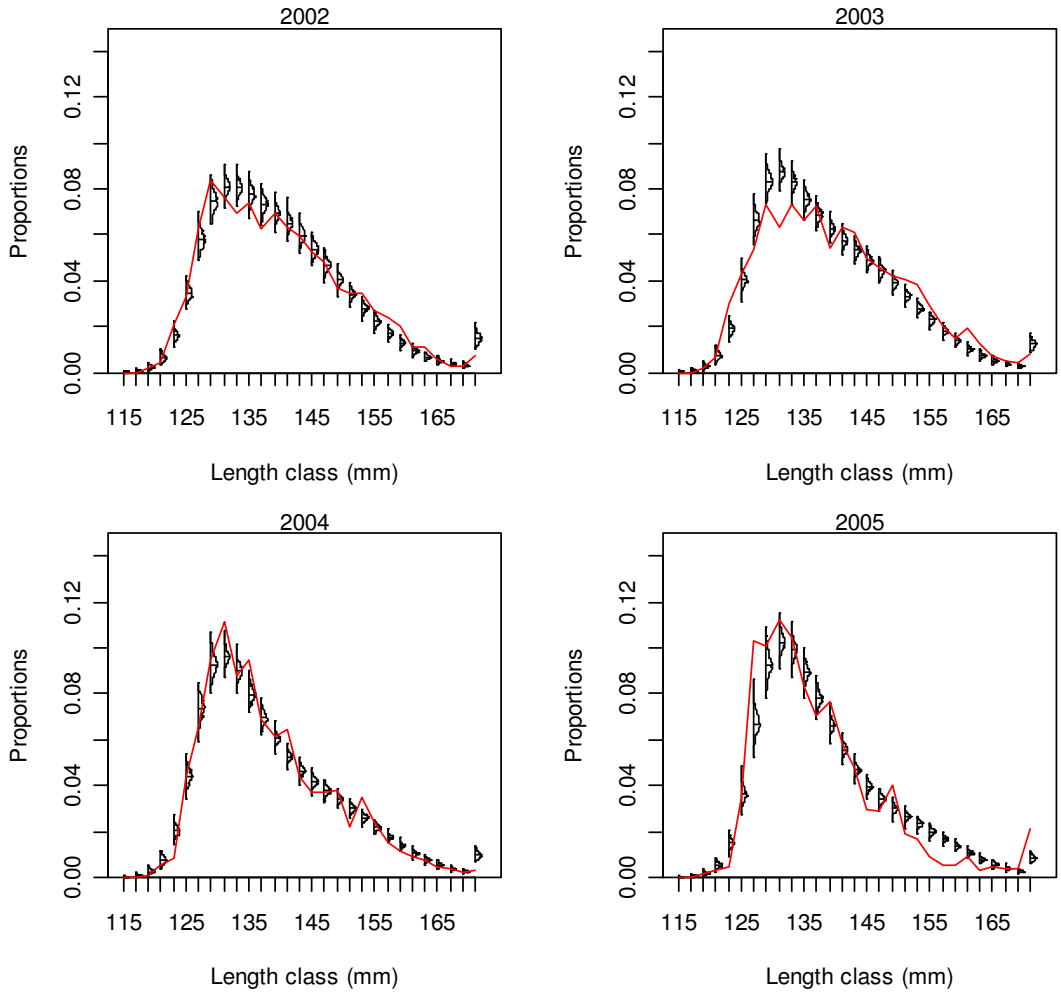

Figure 20: The posterior distributions of the fits to the CSLF data for the base case MCMC. Lines are the observed data.

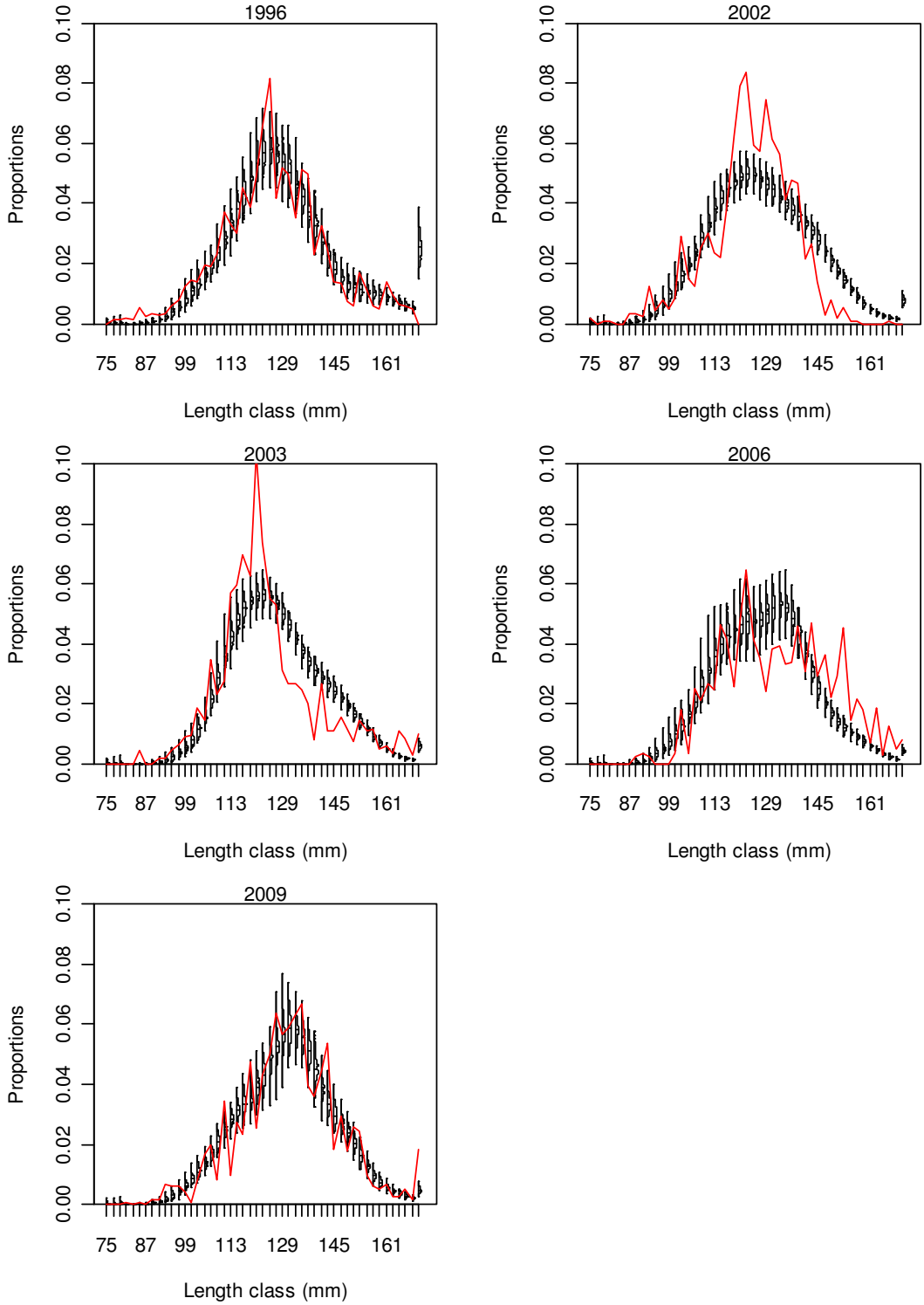

Figure 21: Posterior distributions of the fits to the RDLF data for the base case MCMC. Lines are the observed data.

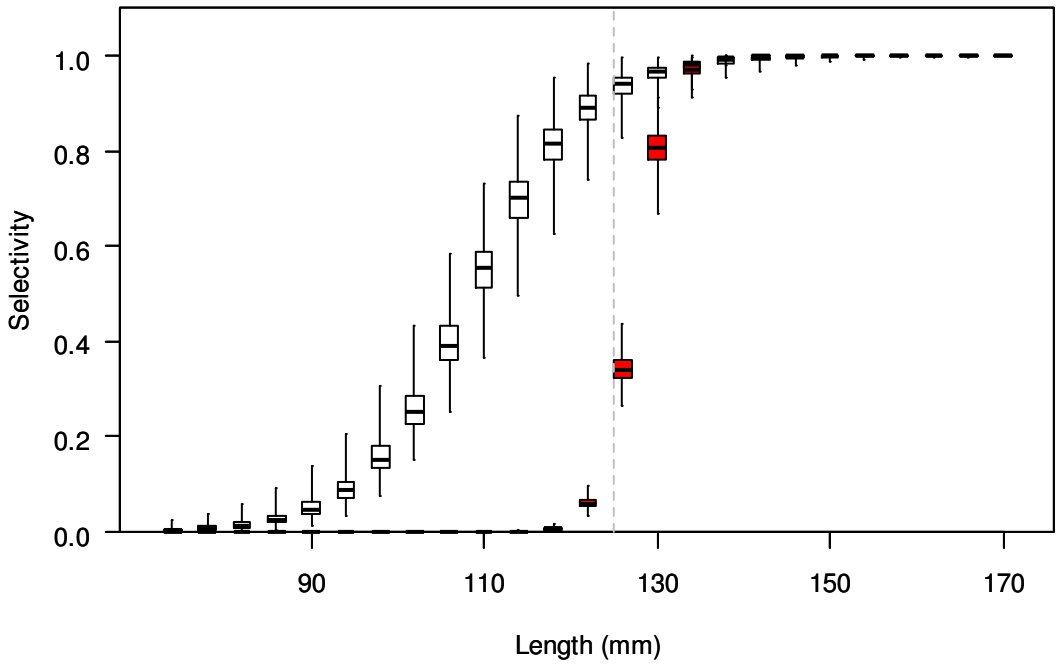

Figure 22: Posterior distributions of commercial (red) and research diver selectivity for the base case MCMC. The box shows the median of the posterior distribution (horizontal bar), the 25th and 75th percentiles (box), with the whiskers representing the full range of the distribution.

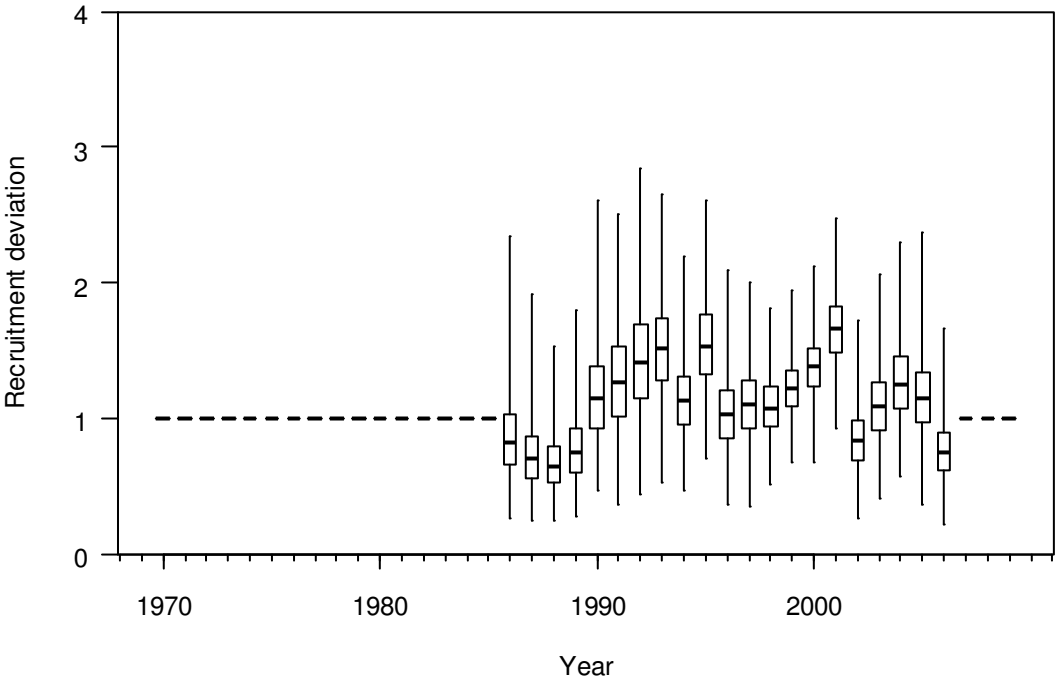

Figure 23: Posterior distributions of recruitment deviation for the base case MCMC. Recruitment deviations were estimated for 1986–2006, and fixed at 1 for other years. The box shows the median of the posterior distribution (horizontal bar), the 25th and 75th percentiles (box), with the whiskers representing the full range of the distribution.

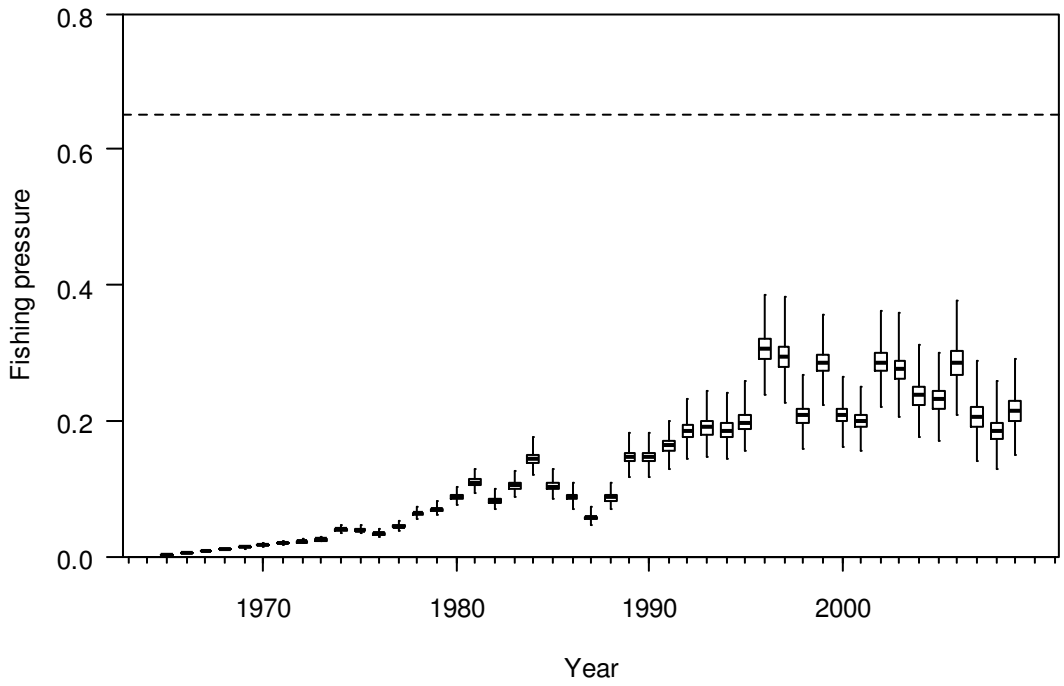

Figure 24: Posterior distributions of exploitation rates (fishing pressure) for the base case MCMC. The box shows the median of the posterior distribution (horizontal bar), the 25th and 75th percentiles (box), with the whiskers representing the full range of the distribution.

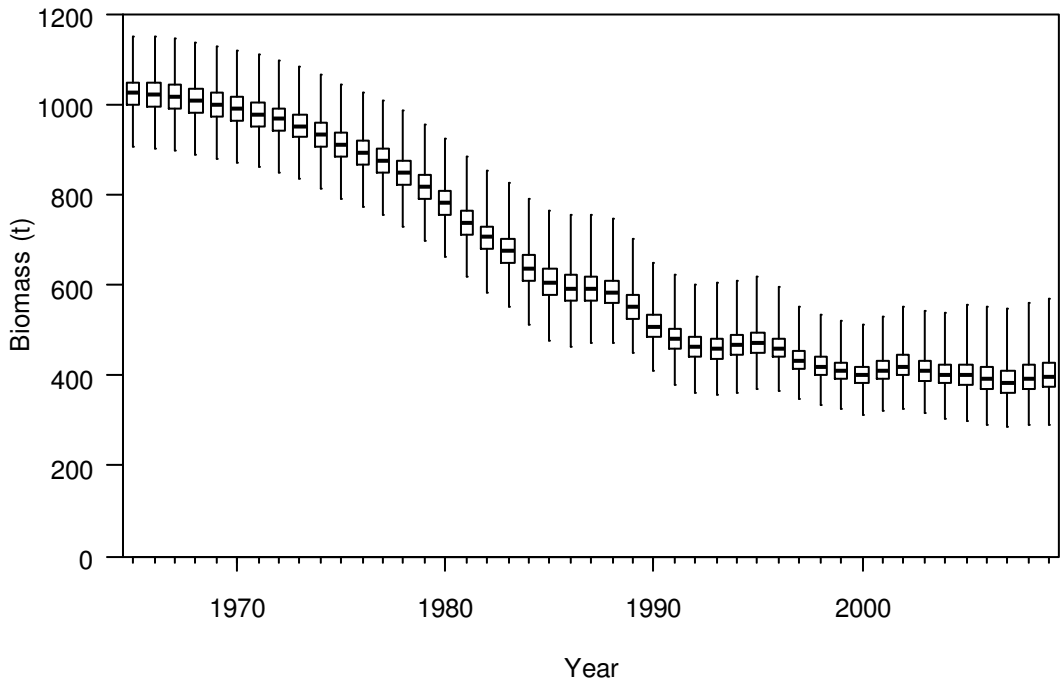

Figure 25: Posterior distributions of spawning stock biomass for the base case MCMC. The box shows the median of the posterior distribution (horizontal bar), the 25th and 75th percentiles (box), with the whiskers representing the full range of the distribution.

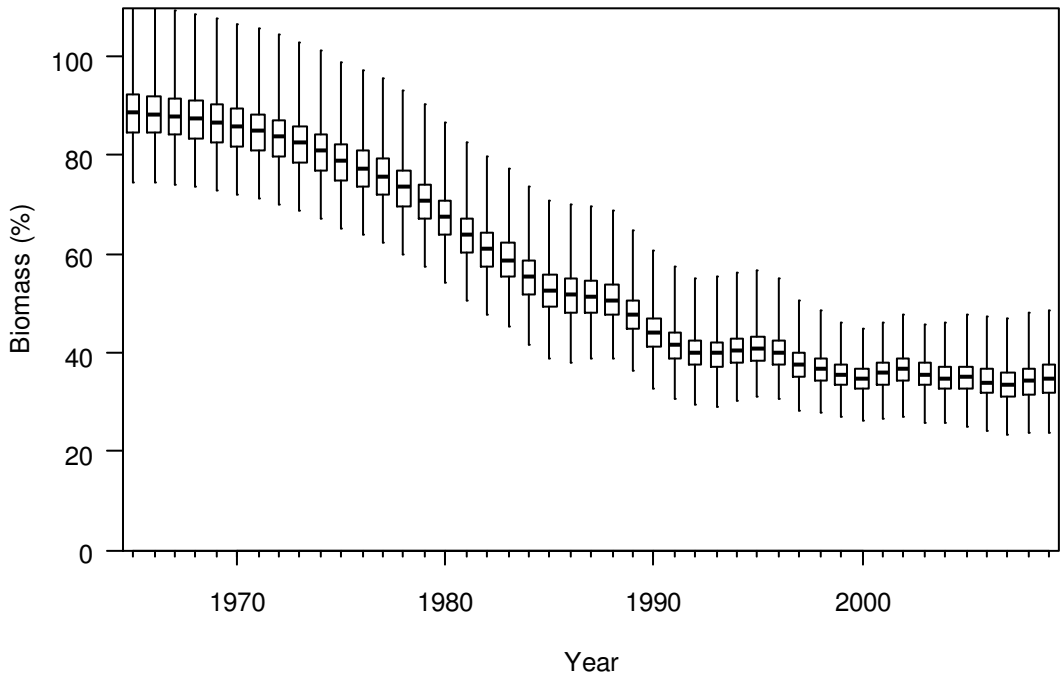

Figure 26: Posterior distributions of spawning stock biomass as a percentage of B_0 for the base case MCMC. The box shows the median of the posterior distribution (horizontal bar), the 25th and 75th percentiles (box), with the whiskers representing the full range of the distribution.

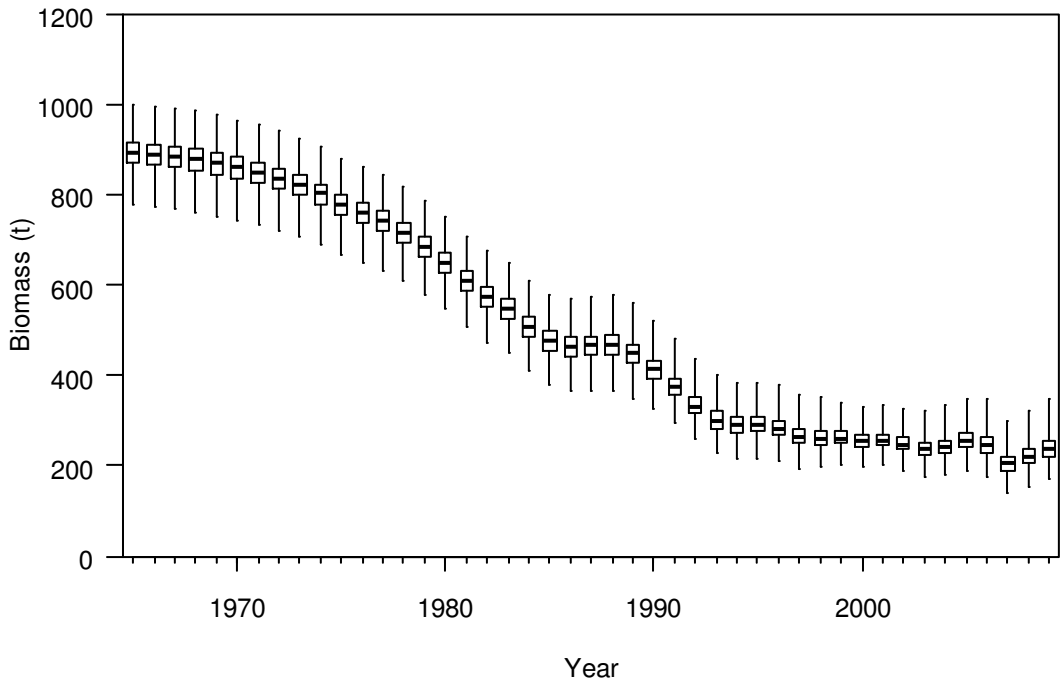

Figure 27: Posterior distributions of recruited biomass for the base case MCMC. The box shows the median of the posterior distribution (horizontal bar), the 25th and 75th percentiles (box), with the whisker representing the full range of the distribution.

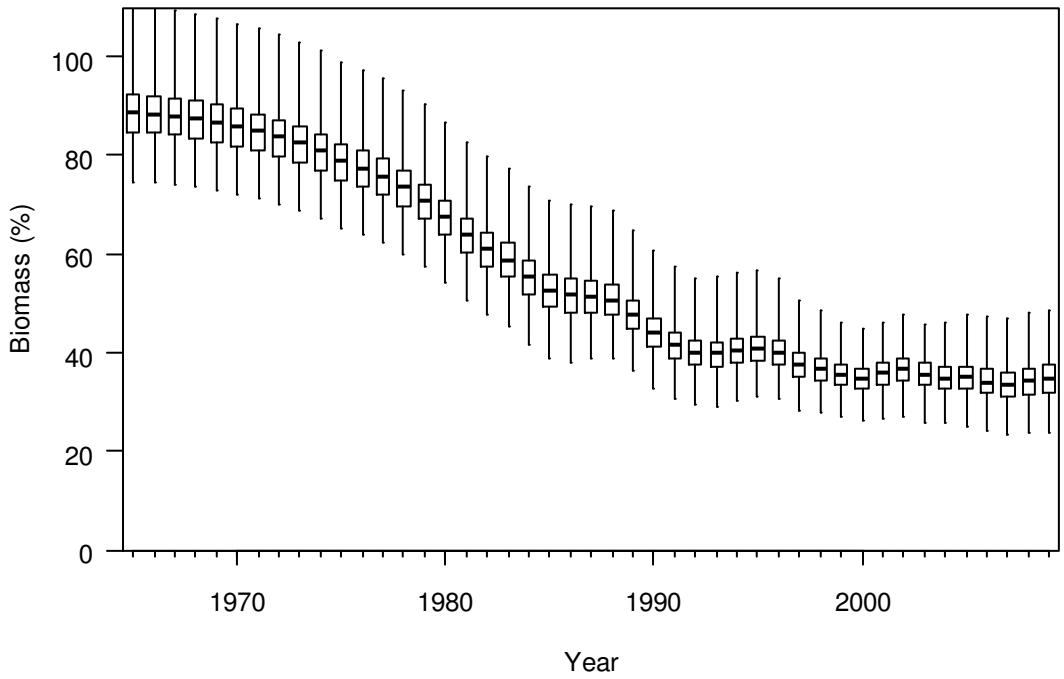

Figure 28: Posterior distributions of recruited biomass as a percentage of B_0^r for the base case MCMC. The box shows the median of the posterior distribution (horizontal bar), the 25th and 75th percentiles (box), with the whiskers representing the full range of the distribution.

APPENDIX A: SUMMARY MPD MODEL FITS

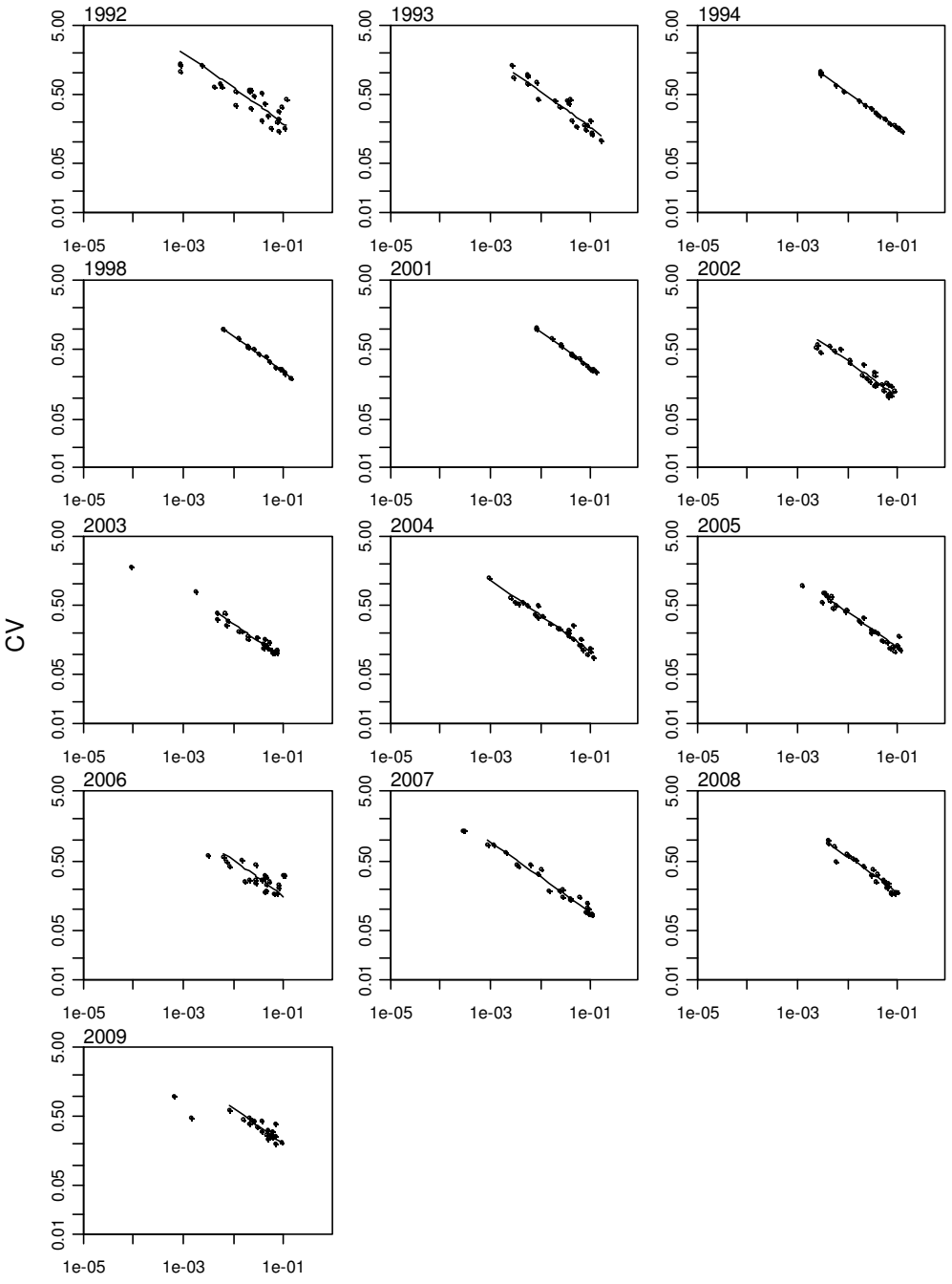

Figure A1: Estimated proportions versus c.v.s for the commercial catch length frequencies for Chalky and South Coast combined for 1991–94, 1998, 2001–09. Lines indicate the best least squares fit for the effective sample size of the multinomial distribution.

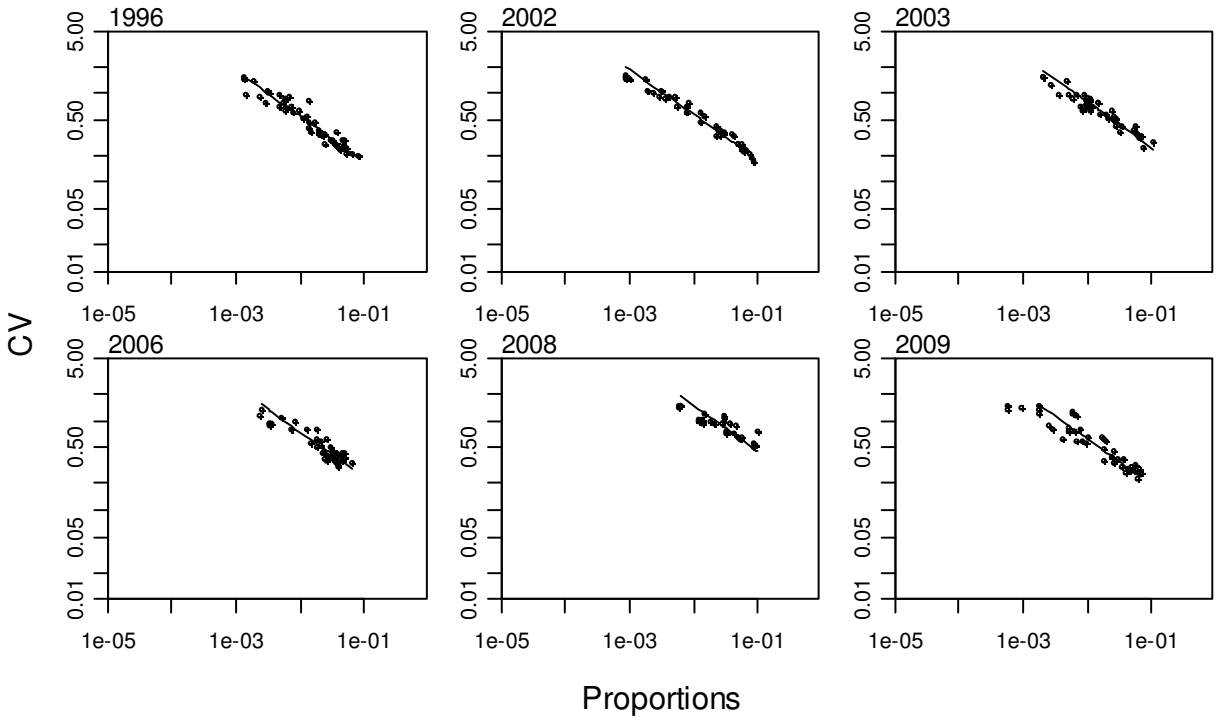

Figure A2: Estimated proportions versus c.v.s for the research diver length frequencies for Chalky and South Coast combined for 1996, 2002, 2003, 2006, 2008, and 2009. Lines indicate the best least squares fit for the effective sample size of the multinomial distribution.

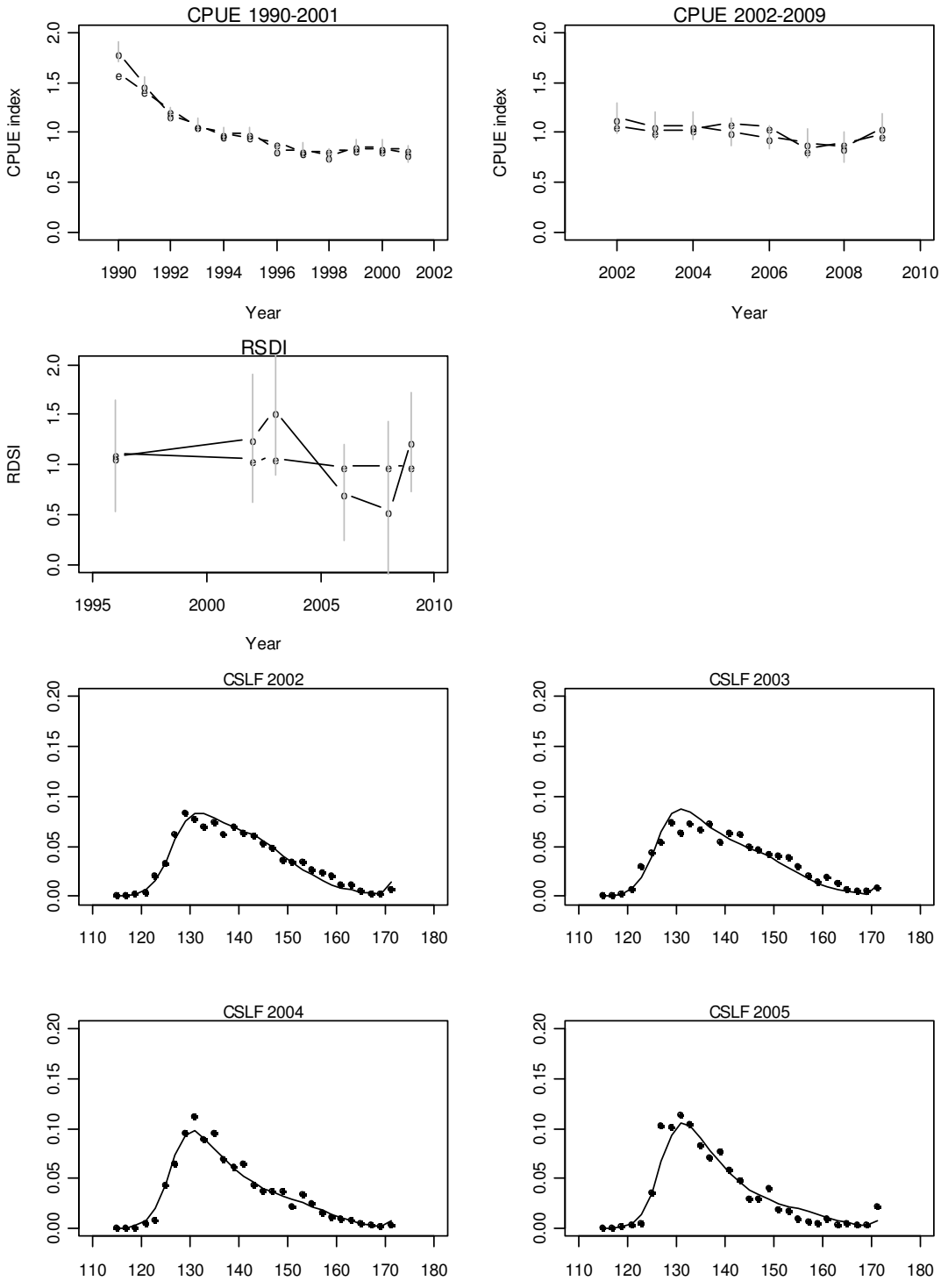

Figure A3: MPD Fits to CPUE, PCPUE, CSLF, and estimated recruitment deviation for sensitivity run 1.1.

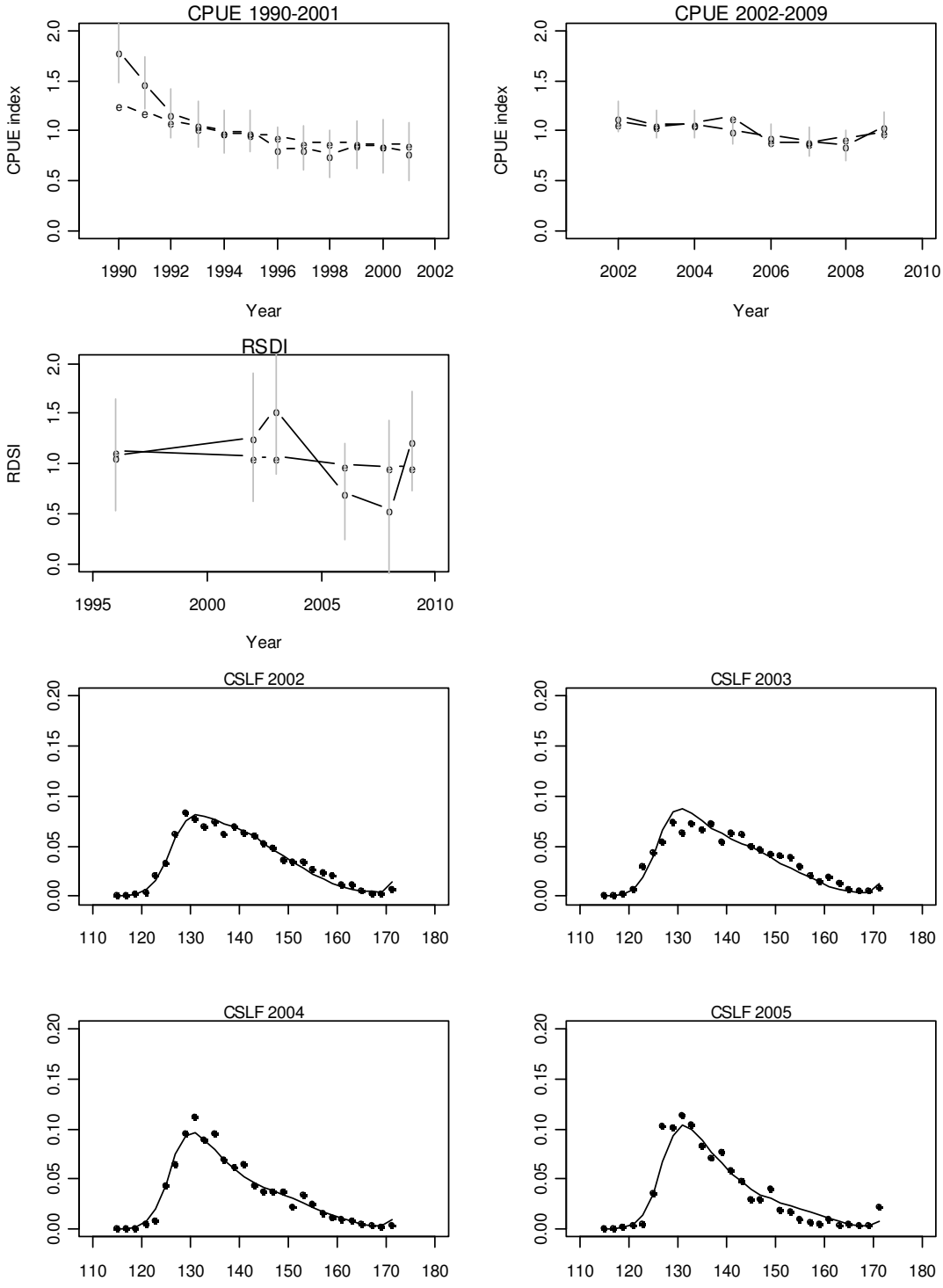

Figure A4: MPD Fits to CPUE, PCPUE, CSLF, and estimated recruitment deviation for sensitivity run 1.2.

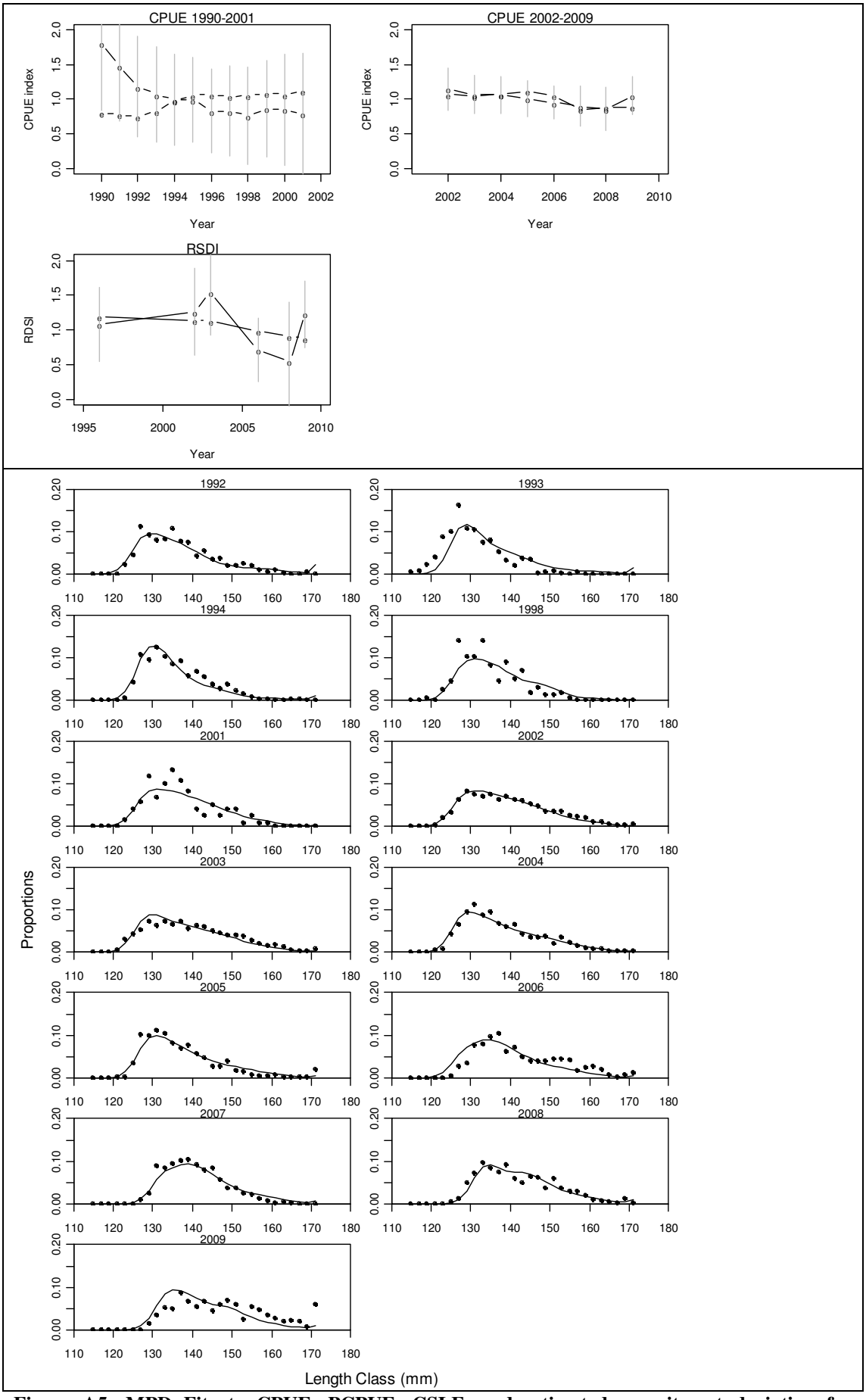

Figure A5: MPD Fits to CPUE, PCPUE, CSLF, and estimated recruitment deviation for sensitivity run 2.0.

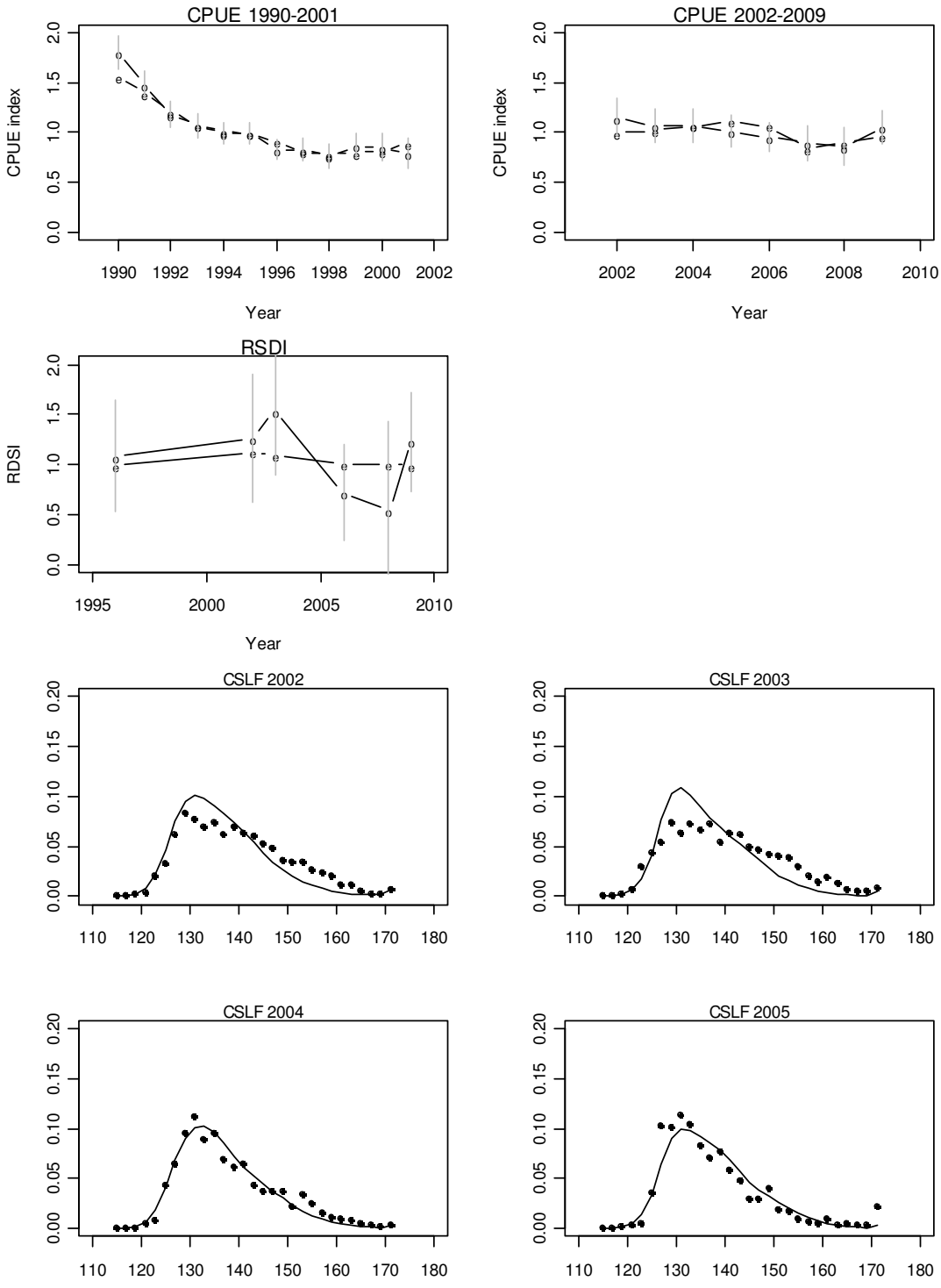

Figure A6: MPD Fits to CPUE, PCPUE, CSLF, and estimated recruitment deviation for sensitivity run 3.0. Note that CSLF doesn't contribute to the total likelihood in this model run.

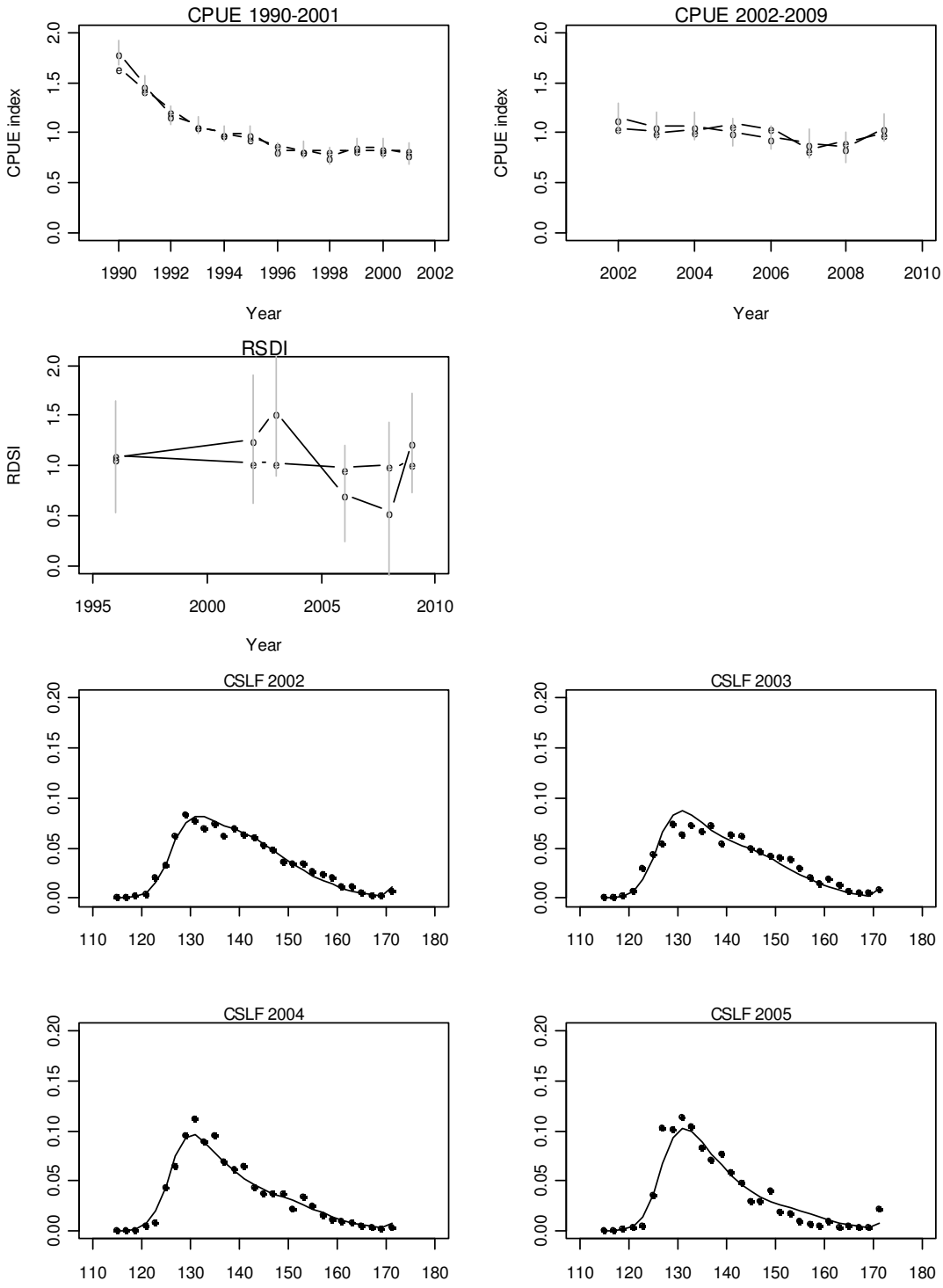

Figure A7: MPD Fits to CPUE, PCPUE, CSLF, and estimated recruitment deviation for sensitivity run 4.0.

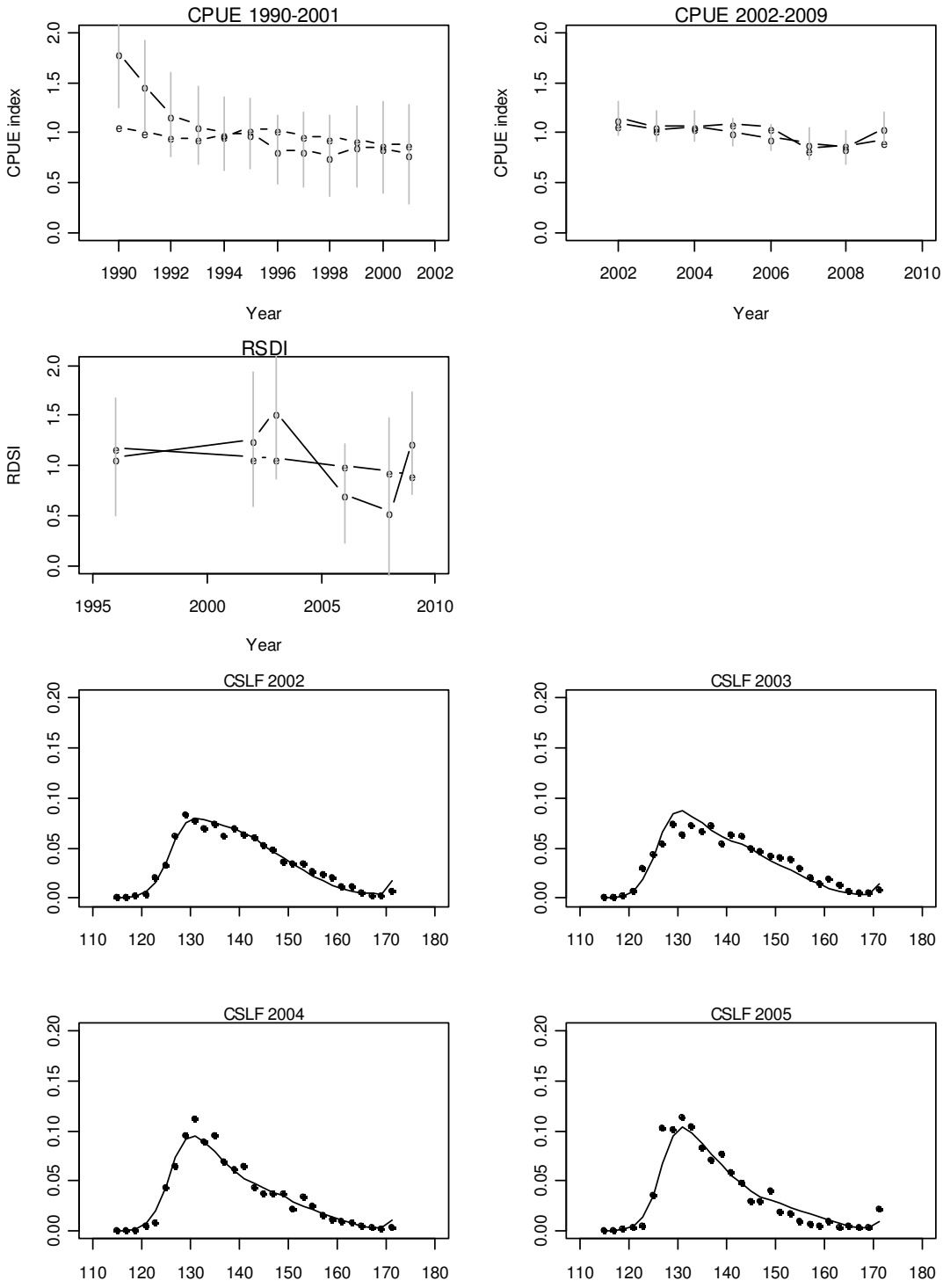

Figure A8: MPD Fits to CPUE, PCPUE, CSLF, and estimated recruitment deviation for sensitivity run 5.0.

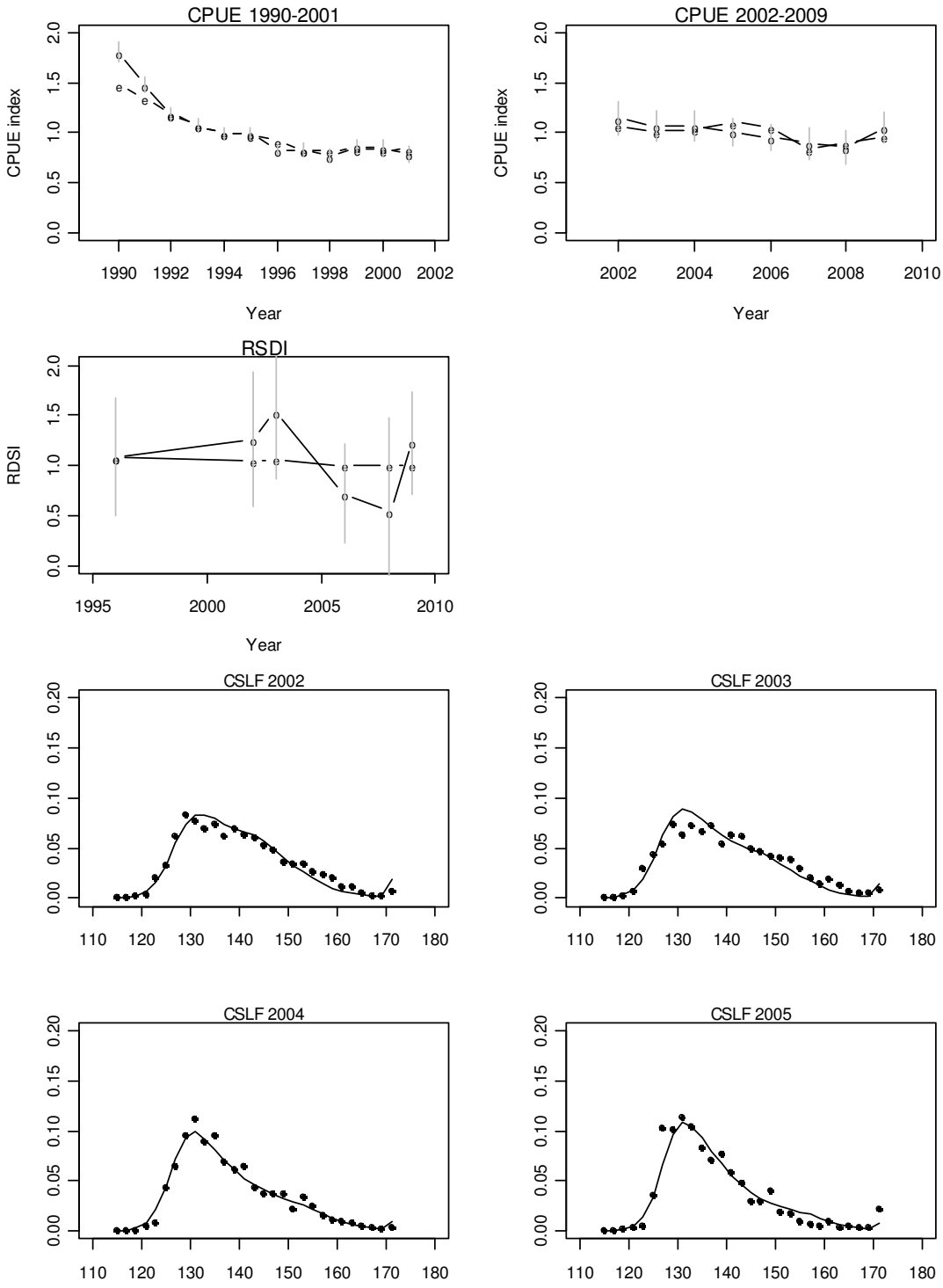

Figure A9: MPD Fits to CPUE, PCPUE, CSLF, and estimated recruitment deviation for sensitivity run 5.1.